Palaeogeography Palaeoclimatology Palaeoecology
February 2022, Volume 587 Pages 110792 (22p.)
https://doi.org/10.1016/j.palaeo.2021.110792
https://archimer.ifremer.fr/doc/00744/85629/

Kilometre-scale coral carpets on mixed carbonate-siliciclastic platforms; a sedimentological study from the Lower Cretaceous of northwestern Africa

Bryers Orrin [1, *], Bulot Luc [2], Duval-Arnould Aude [1], Hollis Cathy [1], Redfern Jonathan [1]

[1] Department of Earth and Environmental Sciences, North Africa Research Group (NARG), University of Manchester, M13 9PL, Manchester, UK
[2] Laboratoire Géosciences Océan (LGO-UMR6538) CNRS - Université de Brest - Université de Bretagne Sud - Place Nicolas Copernic - 29280 PLOUZANE, France

* Corresponding author email address : orrin.bryers@manchester.ac.uk

luc.bulot@univ-brest.fr ; cathy.hollis@manchester.ac.uk ; jonathan.redfern@manchester.ac.uk

Abstract :

Coral carpets are biostromes that form laterally continuous but low-relief (typically less than 1-metre-high) coral communities with a lack of clear internal zonation. There are few locations that allow analysis of such systems on a regional (tens of kilometre) scale in the rock record. This study describes extensive, well-exposed, coral-rich bodies (coral carpets), deposited on the Moroccan northwest Atlantic shallow-marine margin during the Cretaceous (early Hauterivian). The coral-rich sequence reaches 50 m in thickness, with individual carpets between 10 and 100 cm thick, extending over an area of more than 150 km2. Logging and regional correlation, integrated with thin-section analysis, has allowed the evaluation of facies distribution, geometries and temporal evolution. The results provide information on allogenic and/or autogenic driving processes for coral development, and allows the generation of conceptual models for their growth. The Tamanar Fm. corals reflects a shallowing up sequence and the recovery of carbonate productivity following stressed environmental conditions in the late Valanginian. Temporally, coral morphological response relates to high-frequency relative sea level changes that affected water energy and turbidity; thick-branching and massive forms grew in shallow high energy environments whilst platy/flat forms grew in poorly lit and turbid environments. However, local-scale (over hundreds of metres) lateral changes in morphology and facies can be explained by autogenic factors independent of sea level change; varying sedimentation, hydrodynamism and turbidity across the extensive open marine platform.

The termination of coral deposition is marked by a hardground surface, indicating slow rates of sedimentation and a transgression, which is followed by an influx of clastic sediments onto the platform, resulting in the deterioration of carbonate platform health, as conditions became intolerable for coral growth. These coral-rich outcrops contribute to the relatively sparse documentation of Hauterivian corals globally and suggest niche palaeoecological and palaeoclimatic relationships that allowed corals to develop despite stressed platform conditions. The low diversity, low-relief coral carpets may provide a

proxy for the recovery and demise of corals in response to environmental stress on modern carbonate platforms and future climate change projections.

Highlights

► Kilometre-scale coral-rich outcrops onshore the Moroccan Atlantic Margin. ► Non-framework coral carpets show no internal zonation. ► Coral morphology and abundance controlled chiefly by water energy and turbidity. ► Establishment and demise of corals linked to sea level and climatic change. ► Low diversity corals possible proxy for recovery/loss in response to environmental stress.

Keywords : Editor, Isabel Montanez

1. Introduction

The Essaouira-Agadir Basin (EAB) on the western coast of Morocco hosts a well-exposed and highly continuous Lower Cretaceous (lower Hauterivian) carbonate interval. It formed part of an epi-continental carbonate platform that extended around the Central Atlantic during Mesozoic times (Davison, 2005, Fig. 1). Outcrop data (Fig. 1) indicates that the coral-rich beds can be mapped over an area of more than 150 km^2 and extend laterally for over 50 km, and are best described as 'coral carpets'. Coral carpets are biostromes that form laterally continuous but low-relief (typically less than 1-metre-high) coral communities with a clear lack of internal zonation (Tucker and Wright., 1980; Reiss and Hottinger, 1984) and can be either matrix- (non-framework) or skeleton- (framework) supported. They are less studied than reefal build-ups or bioherms and are often overlooked in ancient systems, despite forming a significant contribution to carbonate production and covering greater areas of the seafloor (Riegl and Piller, 2000). Previous work on modern and Mesozoic coral carpets has suggested they grow in warm (typically over 20°C; Fricke and Schuhmacher, 1982) and shallow waters (1-50 m water depths in the photic zone; Riegl and Piller 1997, 2000; Benzoni et al., 2003) and are dominated by scleractinian corals. These corals favour a

hard seafloor substrate and tend to form a veneer on relatively flat seafloor topography (Riegl and Piller 2000; Masse et al., 2009).

During the mid-Valanginian to early Hauterivian, global environmental changes are recorded. A significant perturbation in the global carbon cycle characterised by a positive carbon ($\delta^{13}C$) isotope shift, the Weissert Event, was recorded in the Tethyan (Erba et al., 2004; Mattioli et al, 2014) and Boreal realms (Price and Mutterlose., 2004); and in the Central and South Atlantic (Cotillon and Rio., 1984; Kessels et al., 2006) and Pacific (Aguirre-Urreta et al., 2007). This event has been associated with fluctuations in climate and ocean fertility that affected both shallow and deep marine biota and has been linked with possible ice sheet growth at high latitudes (Greselle et al., 2010; Rogov et al., 2017). The Weissert Event is coeval with the Parana-Etendenka volcanics in South America / Africa (Machado et al., 2018) but it is unclear whether the two events are causally related (Charbonnier et al., 2017; Price et al., 2018;).

Corals exhibit a widespread palaeogeographic distribution during the Hauterivian, which has been ascribed to an increase in global relative sea level (Haq, 2014; Simmons et al., 2020), leading to flooding of continental shorelines. They are documented as isolated biostromes and bioherms in the Lusitanian Basin, Portugal (Rey, 2004), the Provençal platform, SE France (Tomas and Löser, 2008; Masse et al., 2009), northern Mexico (Wells., 1946), the Neuquen Basin, Argentina (Garberoglio et al., 2013), Cerros Perico, Peru (Scott and Aleman., 1984), Benbow Inlier, Jamaica (Löser et al., 2009) and as framework reefs in the Maestrat Basin, Spain (Götz et al., 2005), Paris Basin, Turkmenistan (Bugrova., 1990) and the eastern Black Sea, Georgia (Sikharulidze, 1979). However, these examples do not record aerial distribution and abundance, and the Tamanar Formation of Morocco offers an important contribution to the few comparably scaled modern or ancient examples of laterally extensive coral carpets. This study focuses on the sedimentological context to understand coral distribution and evolution, augmenting most previous studies that often have a more taxonomical approach.

The presence of corals in the Tamanar Formation has been documented in many previous works (Ambroggi., 1963; Duffaud., 1966; Butt., 1982; Rey et al., 1986a and 1986b; Ferry et al., 2007). The aim of this paper is to evaluate the architecture, depositional evolution and extent of early Hauterivian corals, with the aim of providing insights into the evolution and process influencing coral carpet growth, on a multi-kilometre scale. The presence of widespread scleractinian coral carpet communities can offer important information on the palaeogeography and palaeoclimate of a region, and provide broader implications on global climate change and shallow platform conditions. As such, the morphologies and species diversity of these corals can contribute to our understanding of coral evolution during the Early Cretaceous and how it compares to analogous systems in modern and ancient times. Additionally, these coral-rich outcrops are valuable because of their regional scale; giving special insight into how communities change in space.

2. Geological Setting

The Essaouira-Agadir Basin (EAB) is situated on the western coast of Morocco, on the SW flank of the High Atlas mountain range. It is constrained to the north by the Meseta domain, the Massif Ancien to the east and the Souss Basin to the south, which borders the Anti-Atlas Mountains (Fig. 2). The EAB formed as a result of continental rifting during the Permo-Triassic, associated with the opening of the Central Atlantic Margin (Duffaud et al., 1966). Post-rift thermal subsidence from the Early Jurassic until the Late Cretaceous was followed by basin inversion associated with the Atlasic Orogeny (Le Roy and Pique, 2001; Hafid et al., 2006). This reactivated pre-existing syn-rift Triassic and Jurassic extensional structures in a roughly ENE-WSW trend (Hafid et al., 2006). Compression combined with local salt tectonics (Tari and Jabour., 2013; Pichel et al., 2019) resulted in a series of generally E-W trending anticlines and synclines (Fig. 1) which controlled deposition on a regional-scale (Ferry et al., 2007; Luber et al., 2018; Blanco et al., 2020; Charton et al., 2021) andoffer extensive exposure of Cretaceous sediments. The Lower Cretaceous succession is up to 1400 m thick onshore in the EAB, generally forming planar to gently folded outcrops. The succession

tends to thicken to the west (basinward) and units onlap/pinch-out landward in the proximal setting, more than 50 km from the present-day coastline (Rey et al., 1988).

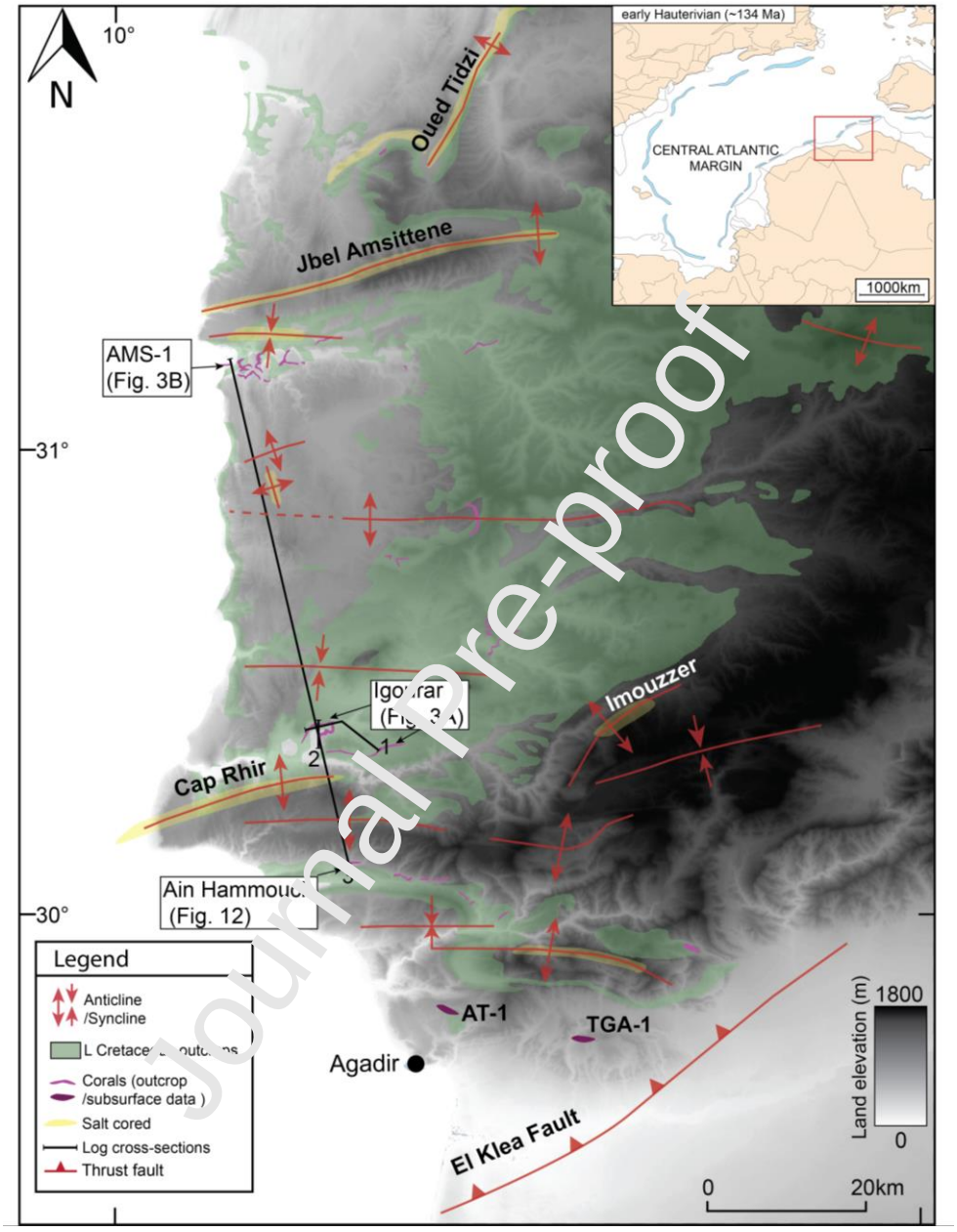

Figure 1 - Onshore Digital Elevation Model (DEM) of the study area showing key structural features (red), presence of salt diapirism (yellow) onshore and location of outcrops (numbered) of the Tamanar Formation across the SW Moroccan margin. Structural data from Hafid et al., (2006) and presence of salt inferred from Tari et al. (2012) and Charton et al., (2021). Subsurface occurrences of corals based on legacy subsurface data (confidential). Minimap (top right) showing palaeogeographic setting during the early Hauterivian (modified from Scotese, 2014) and the positions of major carbonate platforms/shelves (blue shapes) of the Mesozoic that circumvent the Central Atlantic (Jansa, 1981; Davison., 2005: Casson et al., 2020).

Sedimentation during the earliest Cretaceous was carbonate-dominated, with pulses of terrigenous sandstone deposition becoming increasingly prevalent from the Valanginian to the

Hauterivian (Vincent et al., 1978, Fig. 2). Mixed carbonate-clastic successions have been recognised in time-equivalent basins along the Atlantic margin, for example in the Lusitanian Basin in Portugal (Rey, 2004), the Neuquén Basin in Argentina (Zeller et al., 2016) and on the Scotian conjugate (Moscardelli et al., 2019). Although the post-rift setting in Morocco was a passive margin, there is growing evidence of tectonic activity, with significant exhumation and erosion of hinterland Palaeozoic basement structures (Meseta, High-Atlas and possibly Anti-Atlas) throughout the Early Cretaceous, which provided a siliciclastic sediment supply into the EAB with a broadly E-W palaeoflow (Ghorbal et al., 2008; Sehrt, 2014; Gouiza et al., 2017; Luber et al., 2018, Charton, 2020).

This study focuses on relatively undeformed Hauterivian Tamanar Formation outcrops exposed between the Jbel Amsittene and Cap Rhir anticlines (Fig. 1). A generalised stratigraphy is shown in Fig. 2. The formations were originally described by Duffaud et al. (1966); however, their ages were contentious (Rey et al., 1986, 1988; Wiedmann, 1988; Taj-Eddine et al., 1990, 1992; Ettachfini., 1991) until integrated ammonite and microfossil biostratigraphical analysis (Wippich, 2001; Ettachfini, 2004; Company et al., 2008; Luber et al., 2017) confirmed an early Hauterivian age. The Tamanar Formation is made up of massive coral-rich limestones, sandy bioclastic limestones and laminated calcareous sandstones.

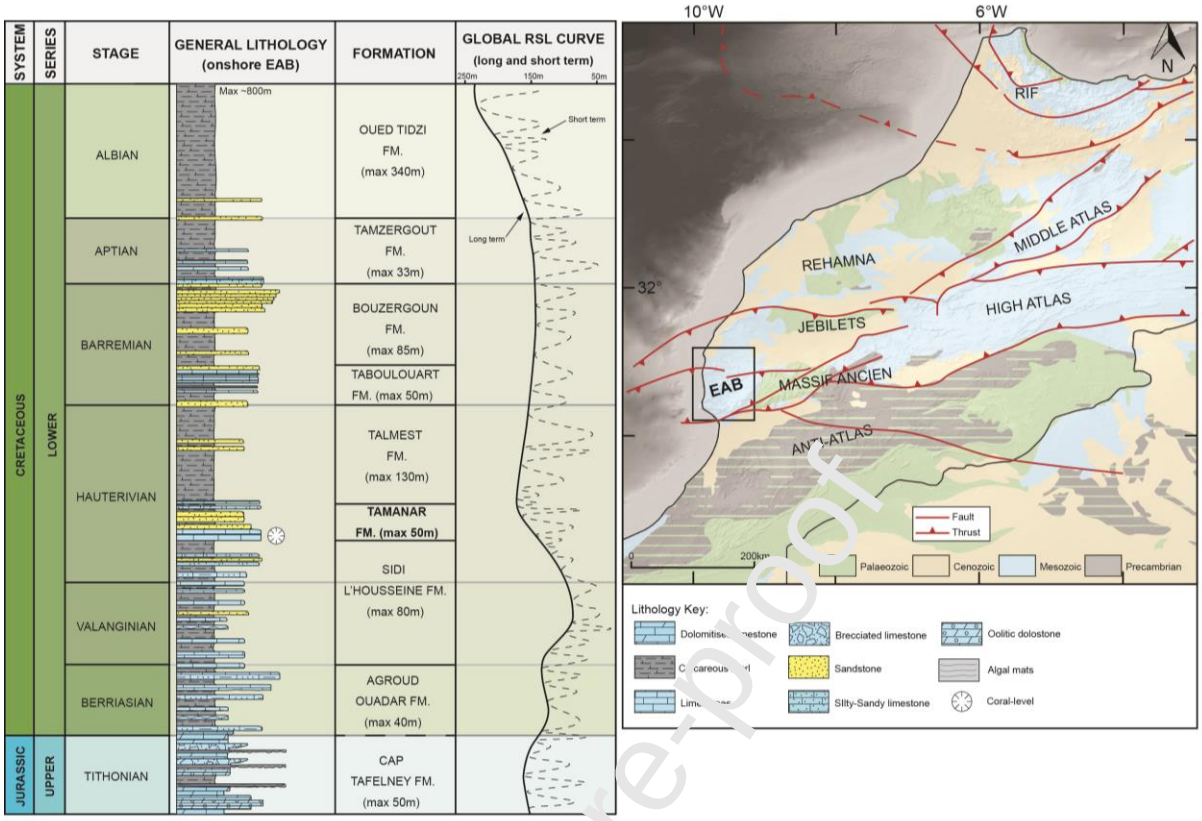

Figure 2 - Stratigraphy of the onshore EAB accompanied by a global sea level curve (Haq, 2014 and Simmons et al., 2020). General lithology was produced using field observations and previous North Africa Research Group (NARG) studies (Luber et al., 2018; Charton, 2021). Map (right) showing the main physiogeographic provinces of Morocco the main cover of sediments and major faults.

3. Methods

The primary method of data collection was through sedimentary logging along a well exposed and laterally extensive outcrop approximately 6 km in length, stretching towards the present-day western Moroccan coastline. Changes in coral growth fabric (sensu Insalaco, 1998) and lithology using Dunham's modified classification (Dunham, 1962; Embry and Klovan, 1971), bed patterns, macro-fossils species and diversity, sedimentary structures, and key surfaces were studied. Each logged section was sampled in the lithologies that contained corals or other notable bioclastic components to allow for thin-section petrographical analysis (fully detailed in *Table S1* in *Supplementary Data)*. Photogrammetry was also implemented where possible to illustrate the changes in beds and the geometry of the outcrop laterally over several kilometres. In total, 11

sections (Table 1) were logged through the Tamanar Formation that range in thickness from 8 to 50 m. Of these 11 sections, 10 were spaced within a 15 km^2 area and one was logged farther from the main study area to allow key surfaces for regional correlation to be walked out; one 3 km to the SE and another 40 km to the NW (Fig. 3). Fifty blue-stained thin-sections were described and approximate skeletal remains, micrite and quartz content, and diagenetic overprint were semi-quantitatively analysed using a microscope. Photogrammetry was used to show the changes in beds and their geometries laterally over several kilometres by stitching photos together to make panoramic images. Extensive sampling was also carried out from the upper part of the Sidi L'Housseine to the lower part of the Talmest formations for biostratigraphic analysis (ammonoids, calcareous nannofossils). Sections were logged from bottom to top and samples of the corals and the rock matrix were taken periodically to allow for microfacies analysis of the individual corals and the matrix sediments. A total of 123 samples were collected. Ammonoid collections made by Ettachfini (2004) were also re-evaluated.

Section ID	Latitude (°)	Longitude	Elevation (m)
TAM1	30.742878	-9.713569	143
TAM2	30.740083	-9.718569	150
TAM3	30.735633	-9.726003	190
TAM4	30.72505	-9.723519	193
TAM5	30.741653	-9.738289	201
TAM6	30.743508	-9.736031	180
TAM7	30.744631	-9.7331	176
TAM8	30.742078	-9.72705	175
TAM9	30.714539	-9.684558	220
TAM10	30.744806	-9.701525	138
AMS-1	31.0977	-9.816494	95

Table 1 – Location and elevation (metres above present day sea level) data for the logged sections.

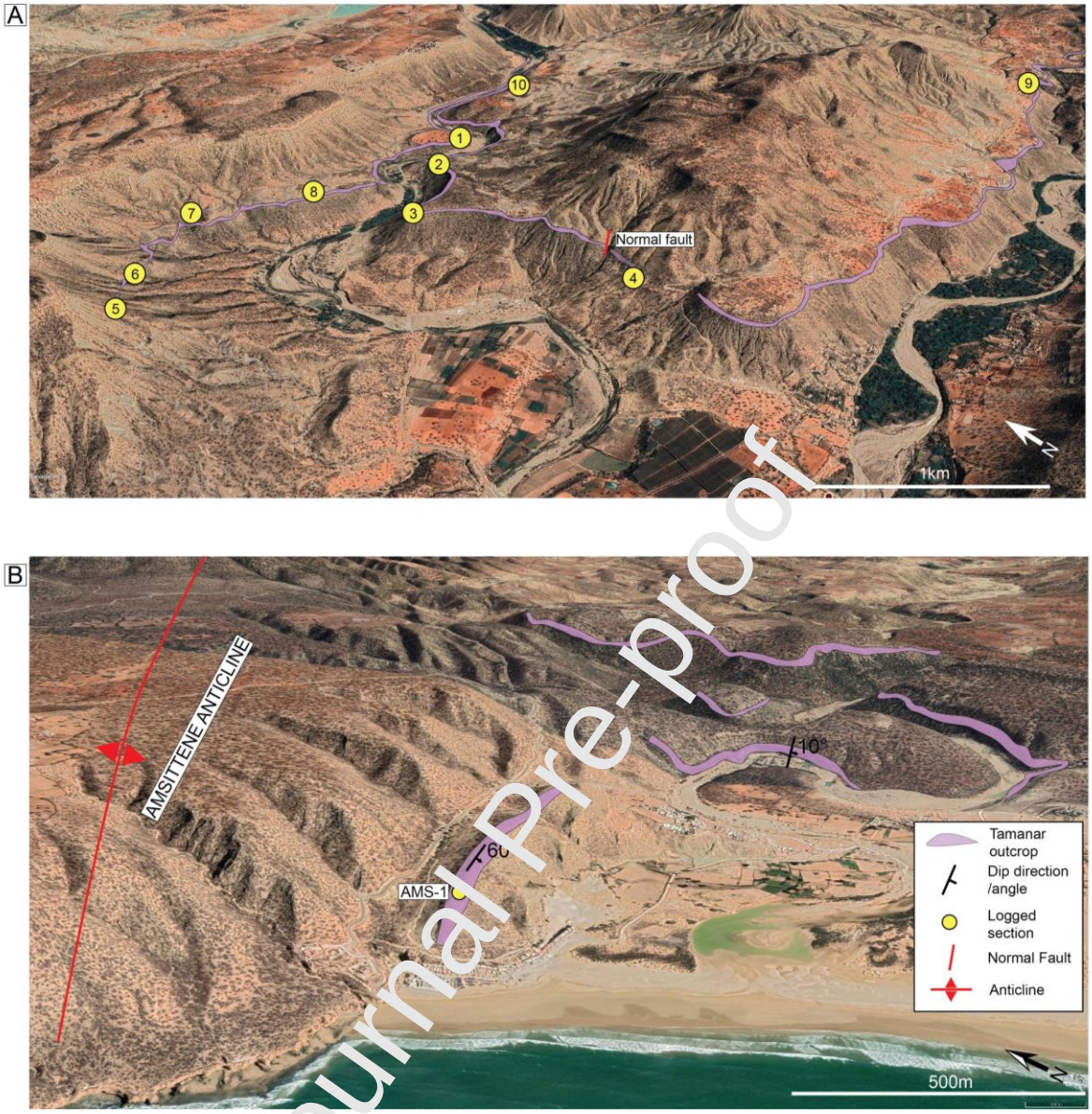

Figure 3 - Google Earth Imagery (2020) showing the locations of the logged sections at Igourar (A) and additionally in the northern EAB (B). Tamanar Formation outcrops are highlighted in a purple shade. Outcrop access and time-constrains permitted one log to be carried out in the section south of Amsittene anticline to allow for regional log correlation.

4. Results

4.1. Facies Associations

Nine lithofacies were observed, defined by texture, fauna, non-skeletal component (silt to fine sand-sized quartz fraction), sedimentary structures and micro-facies (based on thin-section petrography), which can be assigned to five facies associations (FA) based on depositional environments. The inner platform facies association consists of coral domestones (D.1), sandy

packstone to grainstones (B.1), silty wackestone to grainstone (B.2) and oyster floatstones (C). Bioclastic wackestones to packstones (E) are assigned to the inner to middle platform. The coral platestones (D.2) are assigned to the middle platform and calcareous mudstone (F) are assigned to the middle to outer platform. The shoreface facies association consists of bioclastic sandstones (A.1) and laminated sandstones (A.2). Summary lithofacies description for A to F are shown in Table 2. The coral-rich lithofacies (coral domestone, D.1 and coral platestone, D.2), the focus of this paper, are described in detail in the following section.

Lithofacies	Textures	Skeletal Abundance	Sedimentary structures	Bed thickness (cm)	Cementation/ Mineralisation	Non-skeletal component	Facies Association	Process Interpretation	Facies code
Bioclastic siltstone to sandstone	Grain-supported	Oysters (usually at base), serpulids, bivalves, brachiopods, bryozoans, echinoids and small elongated shell fragments	Planar to wavy laminations, moderately to intensely bioturbated top surface (and up to 20 cm below (*Thalassinoides, Trypanites, Skolithos*). Thin fragments orientated NNW-SSE. Sharp and irregular basal surfaces	10-120	Blocky calcite cement, small patches of micrite common, framboidal pyrite rare	Abundant poorly-moderately sorted sub-angular silt to fine sand-sized quartz	Shoreface	Fairly rapid deposition, unidirectional flow, mixing of siliciclastics with wave-reworked bioclasts	A.1
Laminated siltstone to sandstone	Grain-supported	Occasional small shell fragments	Horizontal, wavy and cross-laminations common with moderately bioturbated (thalass', trypanites) top surfaces. Usually sharp based	2-40	Fibrous cement in shell remains, iron oxide crusts on bed tops	Abundant well sorted silt to fine well-sorted sand-sized quartz	Shoreface	Fairly rapid deposition, bi-directional flow with periodic changes in energy leading to ripple migration	A.2
Sandy packstone to grainstone	PST-RST	Oysters, echinoids, gastropods, serpulids, bivalves, brachiopods, bryozoans, coral frags, rare ammonoids	Moderate bioturbation (thalass', trypanites , skolithos) undulating to sharp bases which may have shell lag (usually oysters)	20 to 100	Fibrous to blocky calcite cement and micrite in matrix common, iron oxide minerals in skeletal fragments and crusts	Common sub-angular, poorly sorted silt to very fine sand-sized quartz	Inner platform	Relatively high energy, bioclast reworking and mixing with quartz, intervals of low energy allowing moderate bioturbation	B.1
Silty wackestone to grainstone	WST-GST	Oysters, echinoids, gastropods, serpulids, bivalves, brachiopods, bryozoans, coral frags and rare ammonoids and rare stromatoporoids	Uncommon horizontal lamination in silt-rich intervals, undulating to sharp bases and occassional shell fragment clusters orientated NNW-SSE. Moderate to intense bioturbation (thalass', trypanites, skolithos)	10 to 120	Fibrous (can be syntaxial) , blocky calcite and microspar cement common, iron oxide mineralisations and surface crusts abundant	Common sub-angular and poorly sorted silt-size quartz	Inner platform	Moderate energy, bioclast reworking and mixing with silt-sized quartz, intervals of low energy allowing moderate bioturbation	B.2
Oyster floatstone	MST-WST	Oysters (up to 10cm diameter and thick-shelled)usually fragmentary, serpulids, brachiopods and bivalves	Poorly consolidated and nodular beds common. Moderately to intensely bioturbated (thalassinoides common)	10 to 100	Common microspar cement, iron oxide enriched skeletal fragments and crusts abundant	Common sub-angular and poorly sorted silt-very fine sized sand	Inner platform	Reworked from nearby oyster-banks and deposited in muddy environments during episodic storm events	C
Coral domestone	WST-RST	Densely-packed-branching corals up to 100cm in diameter, dome-lenticular shape). Subordinate undiff' massive shaped corals. Oysters, red algae bryozoans, echinoids, brachiopods, bivalves, serpulids and *Lithocodium aggregatum*, benthic foraminifera	Beds can be continuous or nodular with bases commonly undulating. Can be moderately to intensely bioturbated (thalass trypanites, skolithos) and encrusting organisms common. Non-planar base to individual corals.	10 500	Blocky (can be twinned), fibrous calcite and microspar cements as patches in matrix or in remains, calcite vuggy, iron oxide minerals common,	Uncommon to common sub-angular, poorly sorted silt to very fine sand-sized quartz	Inner platform (well lit, high energy)	Shallow (5-10m WD), moderate-high energy. Corals forming on hard substrates. Changing energy and sedimentation rate allowing varied morphology and varying bioturbation, mixed inter-coral sediment of mud, quartz and reworked bioclasts	D.1
Coral platestone	WST-RST	Similar assemblage to D.1 with platy/ flat corals being the dominant coral and subordinate thin and small ramose branching corals	Beds can be semi-continuous and lenticular with moderate to intense bioturbation and bio-encrustations are common. Non-planar base to individual corals	1 to 50	Blocky (can be twinned), fibrous calcite and microspar cements as patches in matrix or in remains, calcite vuggy, iron oxide minerals common,	Uncommon sub-angular, poorly sorted silt to very fine sand-sized quartz	Middle platform (poorly lit and turbid)	Relatively shallow (10-30m WD) and low to moderate energy, corals forming on hard substrates between muddy sediment. Changing energy allowing varying bioturbation rates	D.2
Bioclastic wackestone to packstone	MST-WST	Oysters, brachiopods, bivalves, serpulids, echinoids, bryozoans, gastropods, rare belemnites, rare small tabular corals and coral fragments	Beds can be nodular and have undulating to relatively sharp bases, slight to intense bioturbation (thalass', skolithos) especially on bed tops	5 to 120	Blocky-fibrous calcite (can be twinned), microspar cement (both in remains and in matrix), vuggy calcite, iron oxide enriched skeletal remains abundant, framboidal pyrite	Uncommon to rare sub-angular poorly sorted silt to very fine sand-sized quartz	Inner to middle platform	Low to moderate energy, bioclast reworking, intervals of low energy allowing bioturbation and larger reworked bioclasts deposited during increased energy (e.g. storm events)	E
Calcareous mudstone	MST	Small oysters, other bivalves, brachiopods, rare ammonoids and undiff' shell fragments and rare nannfossils and forams	No bedding structures and abrupt changes in lateral continuity. Can be nodular in appearance	5 to over 500	Microsparite cement, iron enriched skeletal fragments and nodules common (typically pyrite)	Uncommon to rare silt-sized quartz	Outer platform	Suspension fall-out, pelagic sedimentation and minor disturbances with reworked bioclasts	F

Table 2 – Proposed Lithofacies, key features and interpreted depositional environments. The colour key can be used in conjunction with the logs in Figs. 7- 10.

4.1.1. Coral Domestone (Inner Platform) and Platestone (Middle Platform) Facies Associations

Observations: Facies association comprises two lithofacies; Coral domestone (sensu Insalaco., 1998), D.1 (thick-branched coral wackestone to floatstone) and Coral platestone (sensu Insalaco., 1998), D.2 (platy-rich coral wackestone to rudstone). Beds of lithofacies D.1 have wavy to non-planar basal contacts and are of variable thickness (10 to 400 cm). This lithofacies comprises densely packed phaceloid branching corals (10 to 80 cm thick) that are widely spaced from each other (at least 1 m apart) and are most common in thicker beds (over 50 cm). Massive domal to lenticular corals (up to 100 cm thick) are also found in D.1 without any internal structure preserved (typically filled completely with calcite). Encrusting corals are also found on the top surfaces of beds in lithofacies D.1, these are typically less than 1 cm thick but can extend for several metres laterally. They are dominated by ceroid- corallites (Stylinidae family shown in Fig. 6A) with *astreoid* corallites also commonly found (Fig. 5G). The domal-shaped corals consisting of densely-packed branches (D.1) are widely spaced, with usually over 100 cm lateral spacing between the individual corals. The corals are found upright with contorted bases.

Lithofacies D.2 comprises platy to lenticular (1 to 20 cm thick, commonly *Microsolena*) corals that have a grey to very dark grey colour and are typically more closely spaced (tens of centimetres) than in the coral domestones of D.1. D.2 is limited to thinner beds, 5 to 50 centimetres thick, which can be nodular-bedded with poor lateral continuity. Small (5 cm high and up to 15 cm wide) and delicate ramose corals are also observed as a subordinate morphology and are limited to one locality (TAM9) in a wackestone matrix. Delicate corals (between 8 to 15 cm wide) are also quite widely spaced (more than 50 cm apart). Individual flat to platy corals are found in upright to semi-upright positions with highly contorted basal surfaces, as shown in Fig. 4.

The sediment matrix of the coral domestones (D.1) and coral platestones (D.2) is made up of poorly sorted bioclastic wackestones to packstones (similar to that of lithofacies E)., (50 – 70 %) bioclasts) with abundant echinoids, oysters, other bivalves, brachiopods, serpulids and subordinate bryozoans and gastropods. Benthic foraminifera (mainly texturaliids; *Praedorothia* sp., *Pseudocyclammina* sp., *Protomarssonella* sp. and rare miliolidae (*Meandrospira bancilai* Neagu, 1970) are also observed as subordinate. Although no thorough quantitative measurements were carried out, the field observations suggest that individual corals of both D.1 and D.2 make up approximately 5 to 15 % of the total rock (see Fig. 4 for typical distribution). The matrix of both D.1 and D.2 has a significant portion of micrite (up to 50 % of thin-section optical view), the majority of which has recrystallized within skeletal remains. Rounded to sub-rounded peloids with no internal structure are also common within skeletal remains and small dark-coloured specks with various shapes are also abundant in the matrix and within remains and are most likely iron mineralisations and/or organic matter remains. Both lithofacies also have a highly variable quartz content (0 – 25 % of thin section optical view) made up of sub-angular to angular, poorly sorted silt to very fine sand sized particles. Beds of D.1 have more coral branch debris and skeletal remains (including coral fragments) and are more commonly enriched with iron-oxide, iron hydroxide or iron-sulfide (pyrite) mineralisations (showing an orange-coloured crust in outcrop, in Fig. 5F and a dark orange-reddish colour in thin-section in Fig. 6F) than lithofacies D.2 and is most abundant on bed tops.

Both lithofacies D.1 and D.2 are commonly bioturbated, with abundant *Trypanites* ichnofacies (bivalve borings) shown by circular, sub-circular and elongated pits penetrating the surface of the corals. The borings are commonly filled with fine bioclastic material and/or an iron-oxide/iron-hydroxide or iron-sulfide (pyritic) mineralisation. In D.1, the borings commonly form elongate depressions incising up to 8 cm into the corals (Fig. 5E). The flat/platy corals of D.2 exhibit more bioturbation from their lower and side surfaces than the larger thick-branching and massive corals of D.1 (Fig. 5C) The coral skeletons have been replaced by blocky calcite cements as have some of the skeletal remains in the matrix sediments (in Fig. 6G). In beds that are dominated by

large and thick-branching corals (D.1) coarser skeletal components can be seen (typically a packstone). The intervals with platy corals (D.2) are more commonly associated with a wackestone matrix but can also range into a packstone texture. Corals (both thick-branching and flat/platy morphologies) are encrusted by abundant coralline red algae (in Fig. 6C, *Sporolithon rude*), microproblematic *Lithocodium aggregatum* (in Fig. 6E) and serpulids. Within the coral septa, there is a predominantly micrite or microspar infill. Silt to very fine sized sub-angular to angular quartz grains are observed within skeletal remains, including coral, oyster and microproblematic *Lithocodium aggregatum* fragments surrounded by micrite. Encrustations are predominantly made by *Lithocodium aggregatum* on the upper surfaces of the corals and are also found on the sides of corals (See Fig. 4).

The beds above and below the coral domestones and platestones are most commonly made up of lithofacies E (bioclastic wackestone to packestone), lithofacies F (calcareous mudstone) and occasionally lithofacies C (oyster floatstone), which are described in Table 2. The thinner and more-nodular-bedded muddier intervals host platy/flat corals (platestones; lithofacies D.2) whilst the thicker beds with coarser skeletal components contain the thickly branching and undifferentiated domal corals (domestones; lithofacies D.1). The dominant macrofaunal assemblage (for example oysters, echinoids and serpulids) of the other lithofacies interbedded (within lithofacies E and F with occasional C) with the corals can be variable in a vertical and lateral extent. The beds of limestones of lithofacies D.1 and D.2 lack internal bedding structures but do show a thickening-up followed by a thinning-up trend at several of the sections, where the beds increase from 0.2 metres up to a maximum of 4 metres and then decrease down to 0.1 metres (this, however is not consistent between all the studied localities). The thick-branching and undifferentiated domal corals are spaced widely laterally (greater than 1 metre) and there is no regularity in this spacing (Fig. 4). The platy/flat corals are more typically found as closer spaced communities (10 to 50 cm apart roughly, as shown in Fig. 4) along the same stratigraphic level but can also be found widely spaced like the thick-branching and dome-shapes corals of D.2. Vertically, the individual corals in both the domestones

(D.1) and platestones (D.2) show no clear pattern in their spacing, and they are not observed to come into contact with one another (Fig. 4).

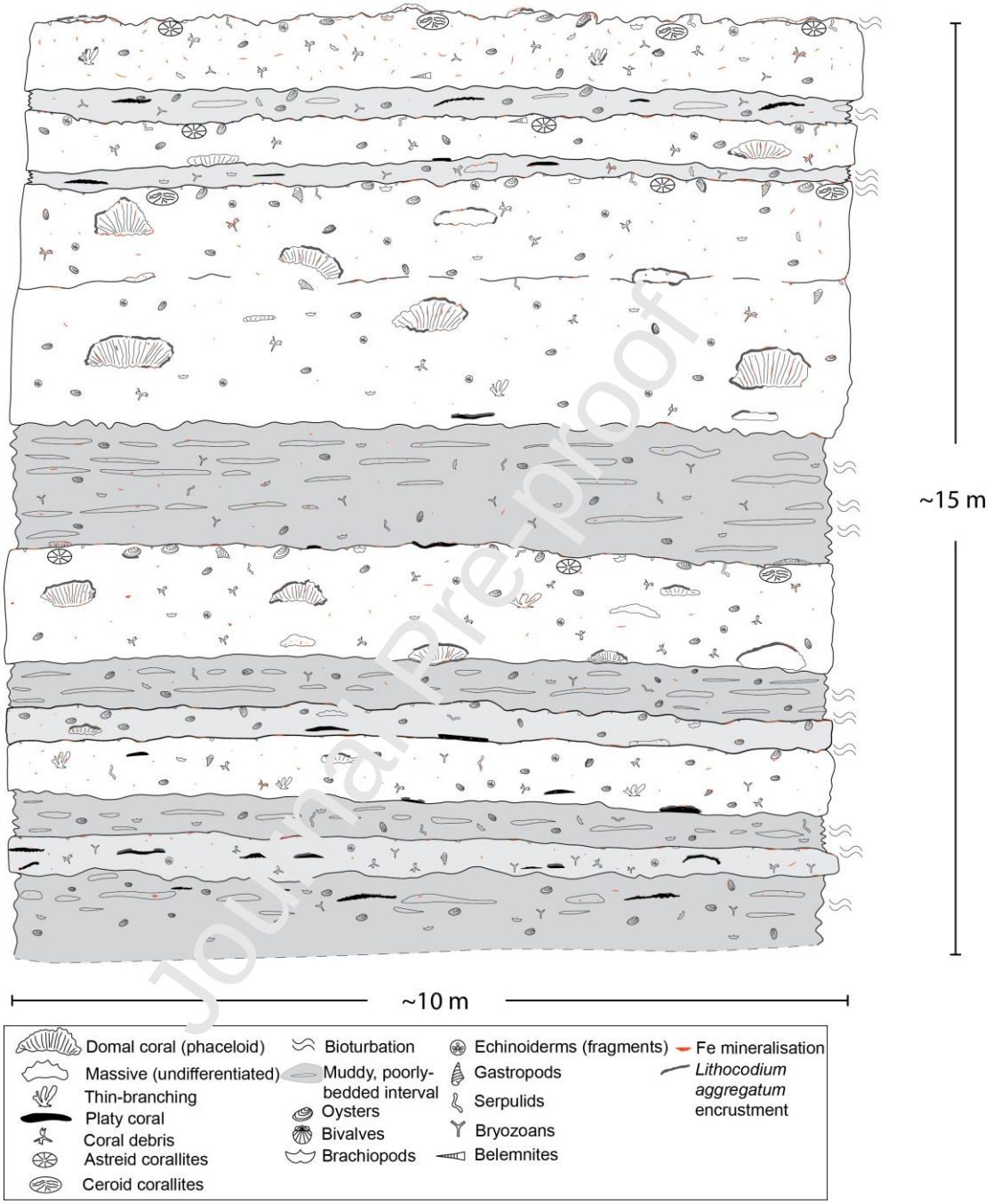

Figure 4 - Typical elementary sequence of the coral-bearing Unit 3 at Igourar showing the approximate distribution and abundance of corals, other notable fauna and sedimentary features. The darker grey colour indicates muddier matrix sediment.

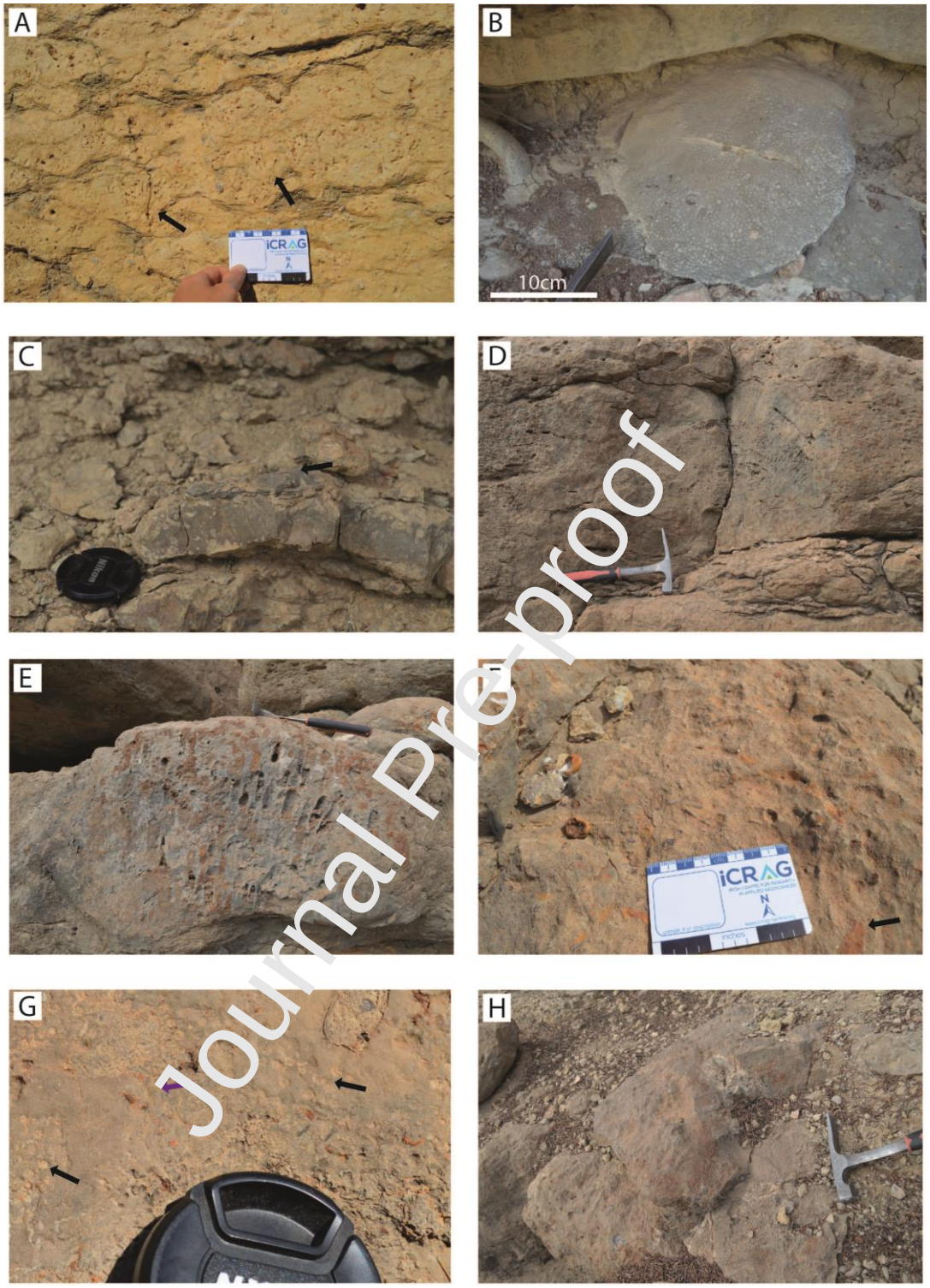

Figure 5 - Key coral morphologies found at logged sections.A - Branching corals (black arrows) held in a predominantly muddy soft sediment full of bioclasts, e.g. oysters, gastropods, brachiopods, serpulids. Small circular pits likely to be bioturbation. Also present is soft-sediment deformation where mud wass compressed by heavier sediment above (Unit 1, TAM9). B – Well preserved large platy/flat-shaped coral found in a micritic interval, facies D.2 (Unit 3, TAM10). C - Platy coral encrusted by an oyster (black arrow) in the nodular-bedded and muddy facies D.2. Bioturbation is also seen at the base of the coral where the surface is more contorted. (Unit 3, TAM8). D – large thick-branching coral (Monastrea?) showing phaceloid structure of corallite, encased in a bioclastic matrix, commonly enriched in iron-oxide, iron-hydroxide or iron sulfide (pyritic) mineralisations (TAM1, Unit 3). E –A large robust coral showing thick and densely packed branches, many of which are bored by bivalves and have been filled with fine bioclast and muds, commonly subject to iron mineralisation (unit 3, TAM8. F – Hardground surface found on the top surface of Unit 3 at TAM7 that is shows borings and

is encrusted by oysters and serpulids which are commonly filled with an iron mineralisation. A branching coral debris is also shown (black arrow).. G – Example of a thin encrusting coral with ceroid (black arrows) and astreoid (purple arrows) corallites at AMS-1. H – Plan view of extensive coral encrustment on a top surface with thick branches of corals visible due to the ferruginous encrustment and corallite infill (Unit 3, TAM8).

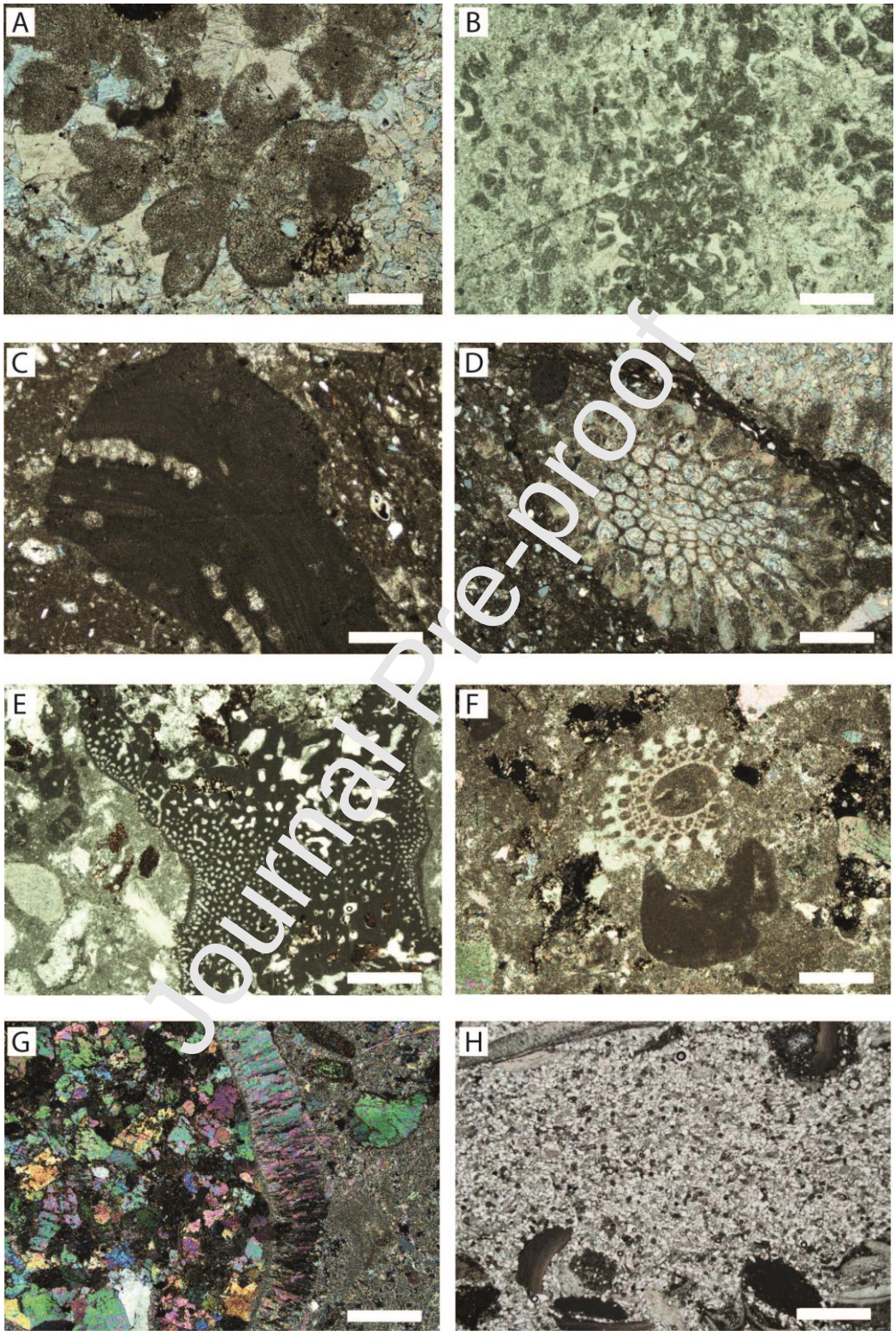

Figure 6 – Thin-section photographs, key biota and early diagenetic features. A – Stylinidae transverse section, internally crystallised by microspar and the coral skeleton has been recrystallised by and blocky calcite (facies D, TAM1 52S). B – Corallites (potentially Stylosmilia?) in transverse section with slightly different morphology, micrite to microspar is prevalent in the internal coral structure and in the matrix (facies D, TAM7 44C). C –coralline red algae (likely Sporolithon rude Lemoine). The matrix is rich in micrite, common bioclastic fragments in which aragonite was replaced with calcite spar and

sub-angular to angular quartz grains (facies D, TAM6 41C). D – Bryozoan showing zooecia which are recrystallised at the periphery with micrite and calcite towards the centre, the matrix is composed of a mix of micrite, scattered quartz and irregular spots of iron mineralisation(facies D, TAM6 41C). E – Microproblematic Lithocodium aggregatum. Several of its sub-spherical cavities are filled with an iron mineralisation, most likely pyrite (facies D, TAM4 44S). F – Echinoderm spine in cross-sectional view, the skeleton has been transformed into calcite and the pores are filled with micrite. The matrix is dominated by microspar with areas of iron sulfide (pyrite) mineralisation (facies D, TAM4 42C). G – Example of the common blocky calcite cementation. The matrix is dominated by micrite to microspar (facies D, TAM7 43S). H – Alternations of bioclastic and quartz-rich intervals (facies A.1, TAM2 61S). White scale bar = 1mm.

Interpretation: the planar geometries, lateral continuity of beds and lack of internal organisation and zonation indicates that Facies Association D formed low-relief non-frame-building communities/coral carpets. on a shallow platform with little topographic relief. Water depth is interpreted as less than approximately 30 metres; e.g. Ricci et al., 2013) for both lithofacies however the domestones (D.1) reflect very shallow inner platform conditions (5 to 10 metres water depth) whilst the platestones (D.2) reflect a slightly deeper (10 to 30 metres water depth) middle platform environment. The thick and tightly packed phaceloid corals in D.1 point to adaptations to a moderate to high energy regime in well-lit conditions (e.g. Leinfelder., 1992; Reolid et al., 2009). The Stylinidae coral family commonly observed on bed top surfaces (Fig. 6) has also been interpreted to reflect growth in relatively high-energy environments (Dupraz and Strasser, 2002). Very similar-shaped and -sized domal corals have been documented in the middle Miocene of southern Turkey and were interpreted as growing in shallow (less than 15 m) moderate to high-energy environments (Vescogni et al., 2014). Platy/flat shaped corals are also often interpreted as an indicator of lower light/higher turbidity environments where the thin yet aerially extensive geometries indicate lateral growth to maximise surface area for incoming light (Rosen et al., 2000; Götz and Löser, 2005; Zawada et al., 2019; Kolodziej and Bucur., 2020). Where abundant in the logged sections, the platy coral morphologies of facies D.2 are predominantly associated with a mudstone-wackestone matrix (lithofacies E), and the high micrite content observed in thin-section and the smaller fraction of fine skeletal debris could indicate a lower energy and/or poorly lit water column. The random orientation of the shelly fossil assemblages in the matrix that are commonly disarticulated and the regularity of coral debris in beds that lack stratification suggests a relatively high-energy environment resulting from wave-action (Kreisa., 1981; Tucker et al., 2003). This is more prevalent in the domestones (D.1)

where the matrix comprises coarser-grained skeletal remains than the wackestone-dominated matrix of D.2. The high lime mud content (represented by micrite infilling skeletal remains and the space between coral branches) could be explained by periodic infilling of porosity as a result of mud settling out of suspension following changes in hydrodynamic energy. Peloids observed within bioclasts appear to be well-rounded and are likely a result of the reworking of carbonate mud (Flügel, 2004).

The abundant microproblematic *Lithocodium aggregatum* points to the presence of microbial crusts associated with the corals. Although its taxonomy is complicated; interpreted as an ulotrichalean green algae (Schlagintweit et al., 2010) or most recently a calcimicrobial crust subject to boring sponges (Cherchi and Schroeder, 2013); it is associated with moderate environmental stress (Flügel , 2004), and has been shown to bind and strengthen coral structures (Weiss and Martindale., 2017). The petrography shows that some of the *Lithocodium* is fragmentary which suggests it was reworked in the matrix sediment prior to deposition. *Lithocodium* has also been strongly associated with warm and shallow water conditions (Schmid and Leinfelder, 1996; Bover-Arnal et al., 2011). These encrusting organisms may have helped stabilise the corals in a moderate to high-energy water column (Leinfelder et al., 1992). Moreover, the benthic foraminifera observed, for example *Praedorothia* sp. and *Pseudocyclammina* sp., are known to be a common feature of shallow inner to outer carbonate platform environments (Koutsoukos et al., 1990).

Echinoderms, predominantly found as debris, are very common in the matrix of D.1 and D.2 and are known to be important grazing and eroding organisms (Mokady et al., 1996; Flügel., 2004). The dominance of filter-feeding heterozoans (oysters, other bivalves, serpulids,brachiopods and bryozoans) in the matrix indicate that the nutrient levels were moderate to high (Hallock and Schlager, 1986; Reymond et al., 2016). The common silt to fine sand-sized sub-angular to angular quartz in the matrix similarly suggests a degree of tolerance to clastics and indicates that the corals had some ability to remove inorganic particles from their surfaces (Lokier et al., 2009). Clastics could

also have been a potential source of nutrients brought along by rivers as suspended matter during periods of increased continental runoff (Sanders et al., 2005).

The non-planar, oyster and serpulid-encrusted, bioturbated and high content of iron mineralisations on top surfaces in beds of lithofacies D.1 and D.2 point to periods of very low sedimentation. The abundant *Trypanites* ichnofacies borings (examples can be seen in Fig. 5D to 5H) point to low sedimentation rates and are associated with sediment-starved hard-grounds in shallow-marine environments (Minter et al., 2016). Platy to flat corals show more bioturbation at their basal and side surfaces and are encased in a muddy matrix which suggests they were adapted to softer substrate conditions than the larger branching and massive corals (Kołodziej and Bucur, 2020).

The high abundance of iron mineralisation and calcite cements show that beds of D.1 and D.2 have clearly undergone considerable early marine diagenesis. The abundance of iron-oxide to iron-hydroxides that have filled the cavities of bioclasts and cover bed surfaces suggests oxic diagenetic conditions which have fluctuated to sub-oxic as evidenced by the common iron sulfides (pyrite) that broke down organic matter during early diagenesis (Carson and Crowley, 1992; Taylor and Macquaker, 2000). The sub-circular scours and pits observed may also have formed from the erosion of soft sediment by increased wave-action (e.g. Bromley., 1992; Pandey et al., 2018). These surfaces show no evidence of sub-aerial exposure in thin section for example vadose zone diagenetic features or pedogenetic features like root traces at the outcrops.

4.2. Biostratigraphy

Even though there is a general agreement about the early Hauterivian age of the Tamanar Fm., its precise extension within that time interval remains poorly constrained. No significant biostratigraphic markers were collected from the Tamanar Fm. itself and its age has to be bracketed by dating of the underlying Sidi L'Housseine and overlying Talmest formations. Unless otherwise mentioned, the biostratigraphic scale retained here is the Standard Mediterranean Ammonite Scale (Reboulet et al., 2018). The upper part of the Sidi L'Housseine Fm. (Fig. 2) is characterised by an

interval of greenish calcareous mudstones that lack macro- or microfossils of biostratigraphic significance. The calcareous nannofossil assemblage is also poor with no clear biomarkers found. The last beds with ammonites occur 50 meters below the base of the Tamanar Fm. and contain an association of Neocomitidae that includes representatives of the genus *Acanthodiscus*. In the Mediterranean Tethys, this genus is restricted to the lowermost part of the Hauterivian, e.g. the *Acanthodiscus radiatus* Zone (Mutterlose et al., 2020). It should also be noted that occurrence of *Acanthodiscus* in the overlying *Crioceratites loryi* auct. Zone cannot be excluded (Busnardo and Thieuloy, 1989).

Rare ammonoids occur throughout the lower part of the Talmest Fm. The oldest specimen (A in Fig. S2) was collected from the very base of the formation close to TAM7 (equivalent to several metres above *KS3* in Fig. 10) and belongs to the newly established genus *Haroella* (Bulot and Pictet, submitted). These taxa are closely allied to *Lyticoceras* distinguished by its quadratic section and sub-adult tuberculated stage. At its type locality (La Charce GSSP, France), it indicates the upper part of the *C. loryi* auct. Zone (*Olcostephanus (Jeannoticeras) jeannoti* Subzone). This is consistent with the report of ammonites from the *C. loryi* auct. Zone at the top of the Tamanar Fm. by Ferry et al. (2007, Ain Hammouch section, Fig. 12). Unfortunately, the ammonite(s) reported by those authors were never named or illustrated and our investigations at the same section failed to collect new material at this level. Slightly higher in the Talmest Fm., an association of *Lyticoceras* gr. *cryptoceras* (including *L. nodosoplicatum,* B in Fig S2), *Olcostephanus (O.) variegatus* and *Plesiospitidiscus fasciger* was collected from section TAM 4 and TAM 8 (several metres above *KS4* in Fig 11). This assemblage unequivocally characterises the lower part of the *Lyticoceras nodosoplicatum* Zone (*Olcostephanus (O.) variegatus* biohorizon *sensu* Bulot et al., 1992). An identical assemblage was collected from the lower part of the Talmest Fm. at the coastal section of Imsouane (Ettachfini, 2004). Above, the ammonite fauna is dominated by coarsely ornamented *Lyticoceras* of the *claveli* group that indicates the upper part of the *L. nodosoplicatum* Zone (*Lyticoceras claveli* horizon *sensu* Ettachfini, 2004).

4.3. Stratal Architecture

The Tamanar Formation was studied in detail at the Igourar outcrop (Fig. 7a and 7b) and at one location south of Amsittene (location shown in Fig. 3b). A detailed log is provided for the Igourar outcrop (log TAM9, the most continuous section in the area, Fig. 8) and for the Amsittene area (log AMS-1, Fig. 9). The Tamanar Formation is constructed of six units, described from base to top:

Unit 1 (coral level 1) is 4 metres thick and marked at the base by a moderately sharp and non-planar basal contact. It is made up of coral-rich limestones with planar to sub-planar bed geometries containing marine fossils: most commonly oysters, brachiopods, echinoids, serpulids, bryozoans and bivalves. At the bottom of this unit, the coral colonies are in-place and quite small (less than 20 cm diameter) and at the base are mainly platy and small branching forms. The following bed contains larger poorly preserved massive dome-shaped corals (D.1) and the top of Unit 1 has a non-planar and burrowed surface which is only observed at the TAM9 section (location in Fig. 3a). Unit 2 is 11 to 12 metres thick and begins with a sharp and highly bioturbated basal contact. It is made up of oyster-bearing limestone beds 20 to 120 cm thick (lithofacies C) with dense shell concentrations at their non-planar basal surfaces that are interbedded with bioclastic limestones of lithofacies E (10 to 50 cm thick) rich in serpulids, bivalves and brachiopods and weathered calcareous mudstones (lithofacies F). At TAM9 these limestones are commonly represented by silt-rich limestones (lithofacies B.2). These are followed by thin (10 to 50 cm) bioclastic limestones (lithofacies E) and silty to sandy limestones (B.1/B.2). The unit then becomes muddier with increasing calcareous mudstones (lithofacies F) with poorly-bedded thin limestones of lithofacies E bearing brachiopods and bivalves. In an approximately east-west orientation (Fig. 7b), roughly in the direction of the modern coastline, Unit 2 is not observed beyond log TAM2. At AMS-1 in the northern part of the basin, Unit 2 is also not observed. Unit 3 (coral level 2) is bound at the base by a non-planar surface and ranges in thickness between 5 to 18 metres. It is made up of a series of massive coral-rich domestones (thickly-branching and undifferentiated massive-shaped corals of lithofacies D.1) and platestones (platy/flat coral dominated beds, D.2) that range from 40 to

400 cm thick. Bed tops of both lithofacies are typically non-planar and bored and/or burrowed with iron mineralisation also very common. In particular, the top surface of Unit 3 is distinctly marked by oyster, coral and serpulid encrustations, abundant borings and burrows and orange to reddish-coloured iron mineralisations that infill borings and cover skeletal remains (usually coral fragments). The surface is easily recognisable in all logged sections and shows sub-circular scours that cut several centimetres into the underlying sediment. This regionally-correlatable bed shows the highest abundance of coral debris and rarely has whole corals in-place within it.

In an east to west orientation (Fig. 7b), the series of massive bedded limestones (dominated by the domestones, D.1) and their distinguishable basal and top surfaces are laterally continuous for several thousands of metres; however, they become thinner and sparser between TAM8 and TAM6 and are interspersed with increasingly thick calcareous mudstones (lithofacies F) and thin beds of wackestone to packstone-textured bioclastic limestones (lithofacies E). From TAM2 to TAM7, in a basinward direction, there is an overall increase in flat/platy corals (D.2) and overall decrease in the large branching and massive corals (D.2). At TAM5 (far left in Fig. 7b) the formation becomes dominated by calcareous mudstones and only thin limestones and sparse coral fragments are observed in beds of lithofacies E. Unit 4 varies from 1.5 to 6 m in thickness and is made up of calcareous mudstones interbedded with poorly bedded limestones (lithofacies E) and rare silt to sand-rich limestones (B.1-B.2). The limestones commonly contains serpulids, bryozoan fragments and oysters. Unit 5 ranges from 3 to 13 m thick and starts with a series of bioclastic wackestones to grainstones that show moderate to intense bioturbation (lithofacies E) and are 10 to 40 cm thick, interbedded with poorly exposed silt-rich calcareous mudstones (lithofacies F). Occasional coral fragments are found in the first bed. These are followed vertically by planar to sub-planar, thinly bedded horizontal to wavy laminated calcareous sandstones (lithofacies A.1 and A.2) interbedded with silt- to sand-rich limestones (lithofacies B.1 or B.2) that show a subtle thickening-up pattern, have sharp non-planar basal surfaces with shell concentrations just above the lower contacts and moderately to intensely bioturbated (mainly *Thalassinoides*) top surfaces. In-place corals are not

observed in this unit at any logged section. Unit 5 is capped with a burrowed and bored non-planar surface encrusted with serpulids, brachiopods and oyster fragments that can be followed between sections. The siliciclastic-dominated interval is laterally continuous; however, decimetre-scale thinning over hundreds of metres can be observed towards the west: the sands (lithofacies A.1/A.2) are thickest in the east (TAM9 to TAM10) where individual beds exceed 1 m but between TAM2 to TAM5 and at AMS-1 they are typically less than 40 cm thick. The elongated bodies of Unit 5 continue past TAM5 to the west, where the coral beds have disappeared, for several hundreds of metres across an inaccessible hillside (shown in yellow in Fig. 7b). Unit 6 starts with a non-planar bioturbated, bored and oyster and serpulid encrusted top surface which is overlain by oyster-rich floatstones (lithofacies C) interbedded with greyish-green calcareous mudstones (lithofacies F) bearing small (less than 1 cm diameter) bivalves and brachiopods. Vertically, the beds transition into silt- to sand-rich limestones (B.1 to B.2) and the calcareous mudstones become progressively thicker. The bioclastic beds contain ammonites (*Lyticoceras* gen. sp. nov.*),* which represent the upper part of the C. *loryi* auct. Zone of early Hauterivian age (see *Biostratigraphy* section*)*. The unit shows a consistent thickness up to the prominent cliff, comprising the Bouzergoun Formation (Luber et al., 2018) across the studied sections in both north-south and approximately east-west (basinward) directions.

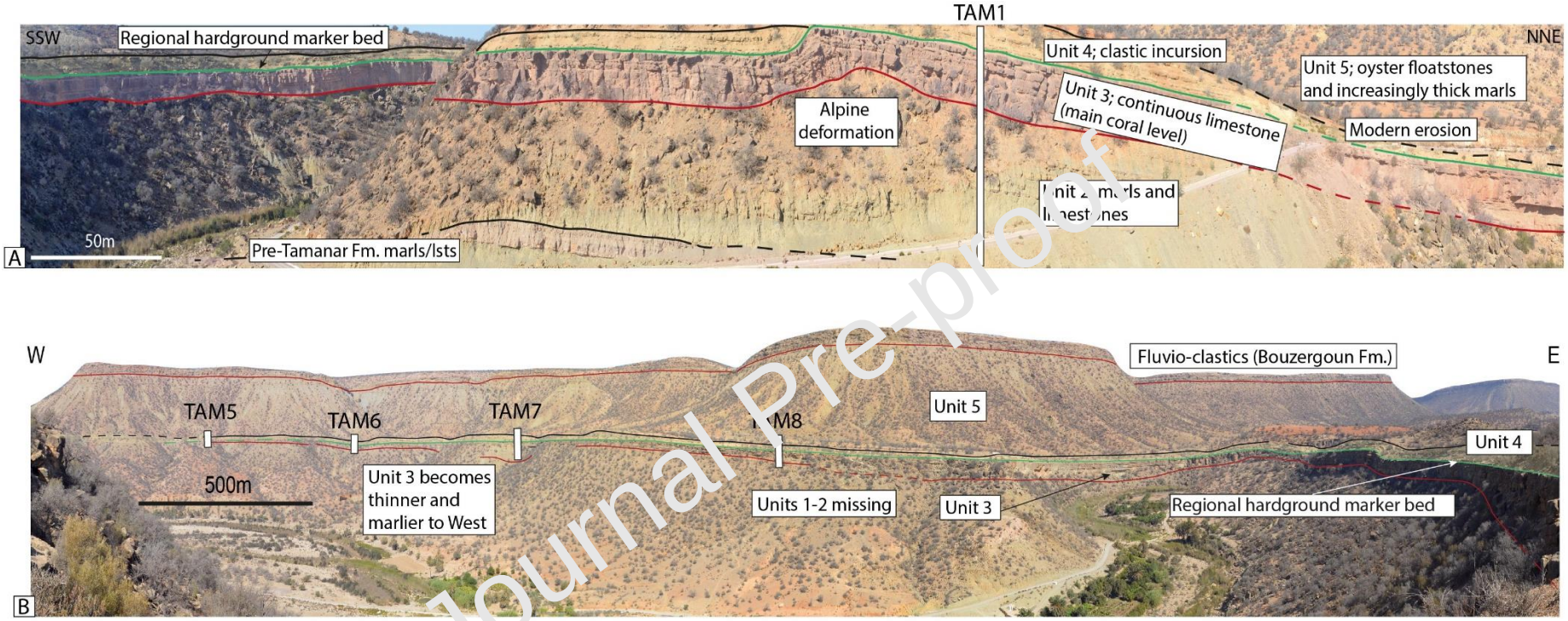

Figure 7 - Large scale geometries of images for logged sections at Igourar. A – photo orientated SSW-NNE in a strike direction in reference to the palaeobasin. B – photo orientated E-W, dip direction towards the west. Unit 3 can be seen to retain a consistent thickness in A. In B, the thickness is also consistent for several kilometres but becomes gradually thinner beyond TAM7 to the west before the formation disappears completely. The area has been subject to considerable modern fluvial erosion that has made the outcrop quality variable.

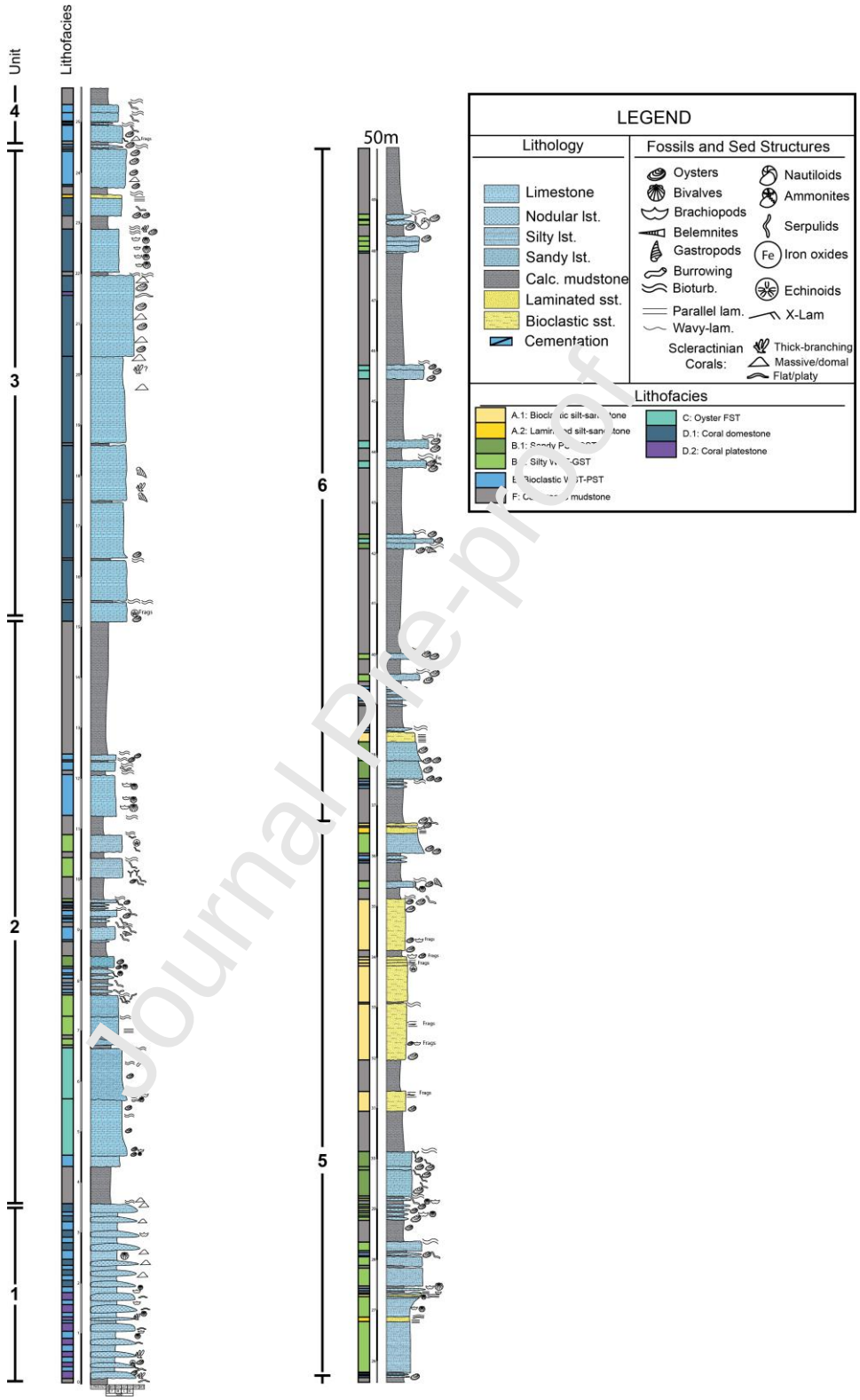

Figure 8 - Igourar Reference Section Log. Section logged at TAM9, the most vertically continuous section logged. It can be subdivided into 6 depositional sequences based on gross depositional stacking patterns and key basal and top surfaces that delimit them.

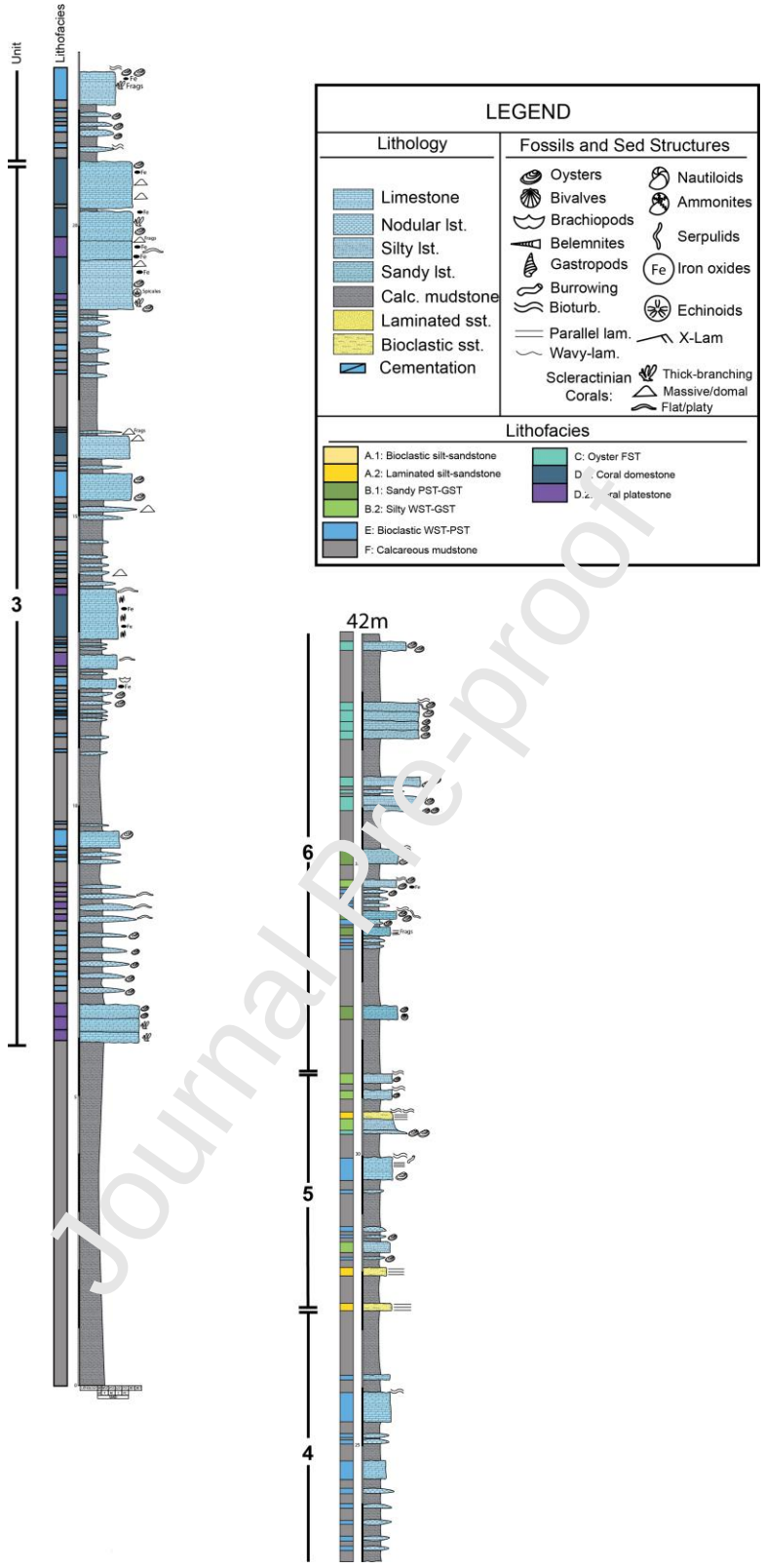

Figure 9 - Amsittene South (AMS-1) Reference Section Log. Depositional sequences 3-6 are recognised based on gross depositional stacking patterns and key basal and top surfaces that delimit them. Sequences 1 and 2 are not observed at this section.

4.4. Sequence Stratigraphic Framework

Sequence stratigraphy is utilised to correlate genetically linked units or "depositional sequences" - in this case sedimentary surfaces, beds and sets of beds (parasequences) - between the studied outcrops on a local (hundreds of metres to several kilometres) to regional (several tens of kilometres) scale.

Coarsening and fining up trends (textural changes from mudstone – wackestone – packestone/grainstone up to floatstone) are interpreted to be a result of changes in water depth and represent high frequency (4^{th} to 5^{th} order, representing tens to hundreds of thousands of years) cycles of relative sea level fall and rise (regression and transgression). A parasequence in this study represents one full cycle of sea level fall and rise (Catuneanu., 2011). Due to the platform's gentle deepening towards the west and lateral facies variations over hundreds of metres, 4^{th} to 5^{th} order relative sea level cycles could not be correlated with confidence between the logged sections because of lateral facies variations; likely a result of local-scale environmental factors discussed later. However, higher order trends (3^{rd} to 4^{th} order relative sea level cycles) were incorporated through the correlation of key surfaces and gross depositional stacking patterns. Surfaces that are irregular due to boring, burrowing and wave scouring, encrusted by marine organisms and are typically covered in iron mineralisations are common in the studied sections. These are interpreted to be hardgrounds that represent periods of very low to zero net sedimentation (Wilson and Palmer 1992). The surfaces show no sign of subaerial exposure and are typically proceeded by fine-grained (MST-WST textures) calcareous mudstones and limestones. They are interpreted as marking the onset of an increase in relative sea level and are most comparable to the transgressive surface or drowning unconformity (Kendall and Schlager., 1981; Christ et al., 2015). In concept, overlying the hardground/transgressive surface should be a Maximum Flooding Surface (MFS) that represents the point of maximum transgression/ the highest stand of relative sea level (Catuneanu., 2011) which may be inferred by deeper water facies proceeding the surface but this is not observed at the studied outcrops, likely due to the variable outcrop preservation.

Irregular and sharp basal contacts are common in the study area and form as a result of subaqueous erosion from current winnowing (Catuneanu., 2006). These basal contacts are interpreted as marking relative sea level fall (regression), with a shift from a deeper to shallower environment.

Key surface 1: The base of the thick-bedded coral-rich limestones (Unit 3, facies association D) records a non-planar, sharp surface resting on the underlying calcareous mudstones deposits (lithofacies F). It can be correlated between all Igourar sections over a distance of 6500 metres and has also been identified 25 km to the north at the AMS-1 logged section. Interpretation: This basal surface likely represents a transgressive surface - it marks a distinct change in facies from the calcareous mudstones to the thick-bedded fossil-rich limestones, potentially signifying a change from a transgressive to regressive system in which relative sea level decreased (Catununeau et al., 2011) on a regional-scale across the EAB.

Key Surface 2: An intensely bored and burrowed, fossil encrusted and ferruginous surface caps the coral-dominated limestones (Unit 3). Sub-circular and elongate scours are observed to cut several centimetres into the hard surface and point to periods of high water energy. The surface is overlain by a thin series of calcareous mudstones and bioclastic limestones (lithofacies E and F). It can be correlated between all the sections (and also recognised in the AMS-1 log, 25 km to the north of Igourar). Interpretation: a marine hardground surface indicating a period of low to non-sedimentation marking the onset of a marine transgression (Kendall and Schlager., 1981).

Key Surface 3: A non-planar, sharp surface marking the contact of calcareous mudstones with sand-rich beds. Interpretation: Similar to KS1, it is interpreted as marking a relative sea level drop, with a move from a relatively deeper platform (lithofacies F and E) to a shallower shoreface environment (lithofacies B.1, B.2 and A.1-A.2). It is partially correlatable between the Igourar sections on a local-scale and tentatively on a regional-scale from TAM9 to Ain Hammouch and AMS-1.

Key Surface 4: A non-planar, heavily burrowed (*Thalassinoides* ichnogenus) and bored (*Trypanites*) surface that caps the sand-rich Unit 6. *Thalassinoides* suggest relatively soft and sandy sediment. Key surface 4 marks termination of the calcareous sandstones (FA-A, shoreface environment) and change to silty to bioclastic limestones (B.2 and E) to the oyster floatstones (C) and silt to sand-rich packestone-grainstones (B.1) interbedded with greenish calcareous mudstones (FA-B, outer platform environment). It can be correlated between the logged sections where the outcrop is not removed by modern erosion. Interpretation: A marine firmground surface,dissimilar to the hardground KS2 as it is not extensively encrusted or bored or cemented and therefore not interpreted to have developed into a fully lithified hardground (Christ et al., 2015).

4.4.1. Local Correlation

The ten measured sections at Igourar span a lateral extent of six kilometres. Correlations were made based on defining units, their internal facies and, where possible, the bounding surfaces that separate them. To the west of section TAM9, at TAM10 (right side of Fig. 10), Unit 1 cannot be correlated as the outcrop seems to be buried under the riverbed and it does not outcrop at TAM1 or any other sections. Unit 2 can be correlated solely between TAM9 and TAM1 and Unit 1 was not observed elsewhere from TAM9. Lateral facies variations are clearly observed in Unit 3 from roughly east to west with, for example, lithofacies D.2 transitioning into lithofacies C between TAM6 and TAM7 (left side fig. 10), from coral platestones to oyster floatstones. Another clear example is observed in a basinward direction between TAM2 and TAM8 where beds are dominated by thin platy corals (platestones, D.2) at TAM8 rather than larger thick-branching and massive ones (domestones, D.1) at TAM2. The facies composition also varies in a north-south direction, for example being more mud-dominated (lithofacies F) at TAM7 compared to TAM4 which is 1000 metres to the south (fig. 11). Changes from D.1 (domestones) to D.2 (platestones) are observed within Unit 3, evident for example between TAM2 to TAM8 (Fig. 10). The lower part of Unit 3

thickens from TAM1 to TAM2 where a further 7 metres of coral-bearing beds (D.1 and D.2) are observed below the distinguishable thicker-bedded upper part of Unit 3 (See TAM2 on Fig. 10). Unit 4 increases in thickness towards the west (between TAM8 and TAM5 in Fig. 10) and the calcareous mudstones (lithofacies F) become thicker and the bioclastic limestones (lithofacies E) become more nodular-bedded. In a proximal (east-west, from TAM8 to TAM9 in Fig. 10) direction Unit 4 is very thin (decreasing from 6 to 1.5 m). Unit 5 also displays lateral shifts in facies over hundreds of metres, for example between TAM2 to TAM7, the silty to sandy limestones (facies B.1/B.2) shift into laminated and bioclastic sandstones (A.1/A.2) and then transition back to the silty to sandy limestones (Fig. 10). Unit 6 is uniform between the logged sections. Oyster-rich beds (lithofacies C) and ammonites-bearing silty to sandy limestones beds (lithofacies B.1/B.2) can be clearly followed between logged sections (top of fig. 10 and top of Fig. 11). No clear lateral facies variations within Unit 6 are observed in east-west or north to south directions at the Igourar outcrop.

Changes in thickness, for example the loss of the thicker beds between TAM2 and TAM8 (Fig. 10) and TAM4 to TAM3 (Fig. 11) could be related to varying accommodation space as a result of differential subsidence, as could the absence of Unit 2 beyond TAM1 and the localisation of corals in Unit 1 to TAM9. Small-scale (over hundreds of metres) changes in accommodation space related to changes in bathymetry would affect sedimentation rates and coral morphology with changing turbidity. However, this cannot explain the changes in coral morphology and lateral facies variations where no significant thickness variations are observed.

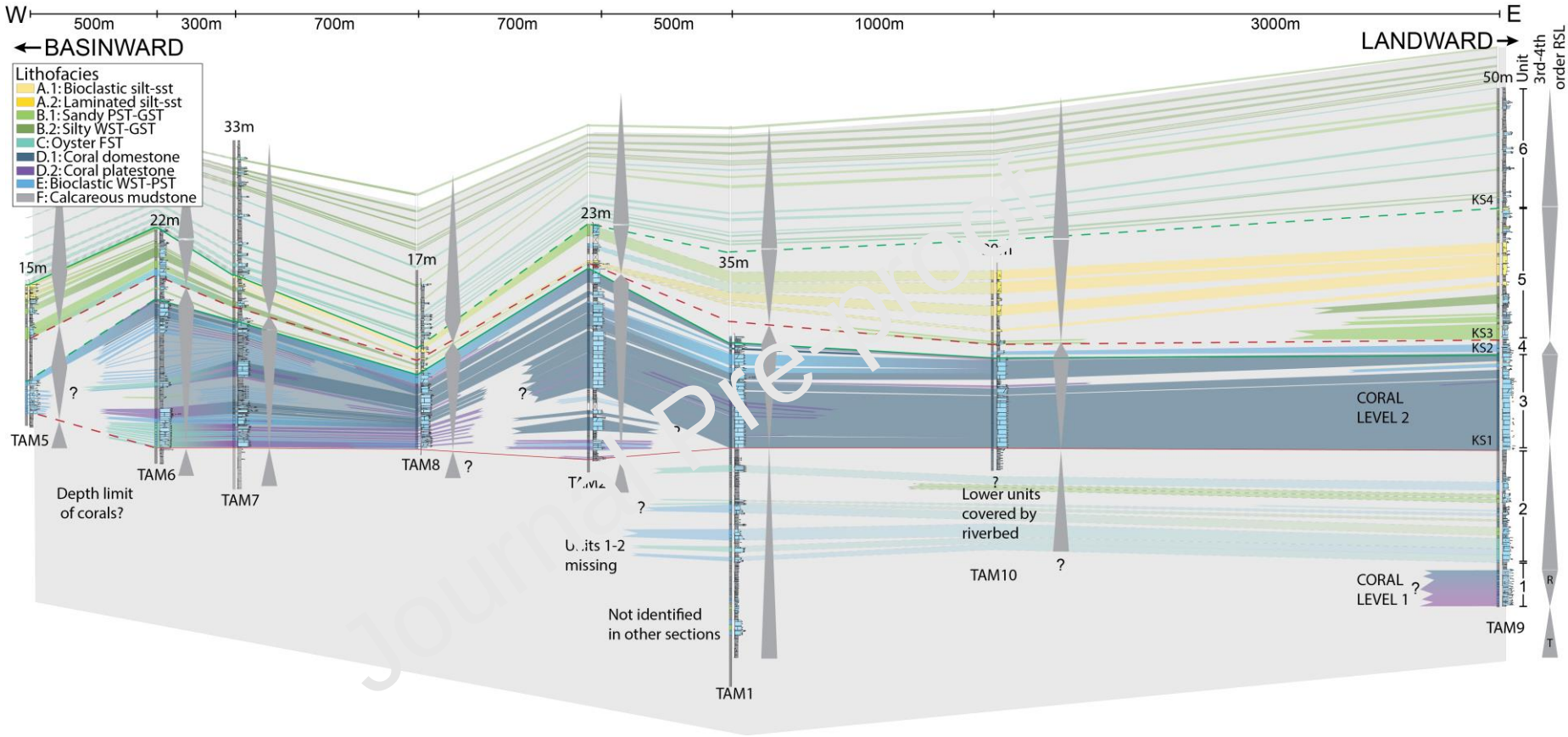

Figure 10 - Log Correlation Local East-West (line 1 on Fig. 1). Datum is the base of Unit 3 (KS1). Correlation of depositional sequences and sequence stratigraphic surfaces in direction of basin (west) based on the logged sections in the Igourar location. Green line – transgressive surface, red line - regressive surface and dotted lines infer tentative correlation between sections. Geometric relationships are exaggerated (e.g. between TAM2-TAM8) most beds are horizontal to sub-horizontal in the field. Lighter shades for facies indicate inferred facies where there was lack of outcrop data due to modern fluvial erosion. 3rd to 4th order relative sea level cycles are also interpreted at each section.

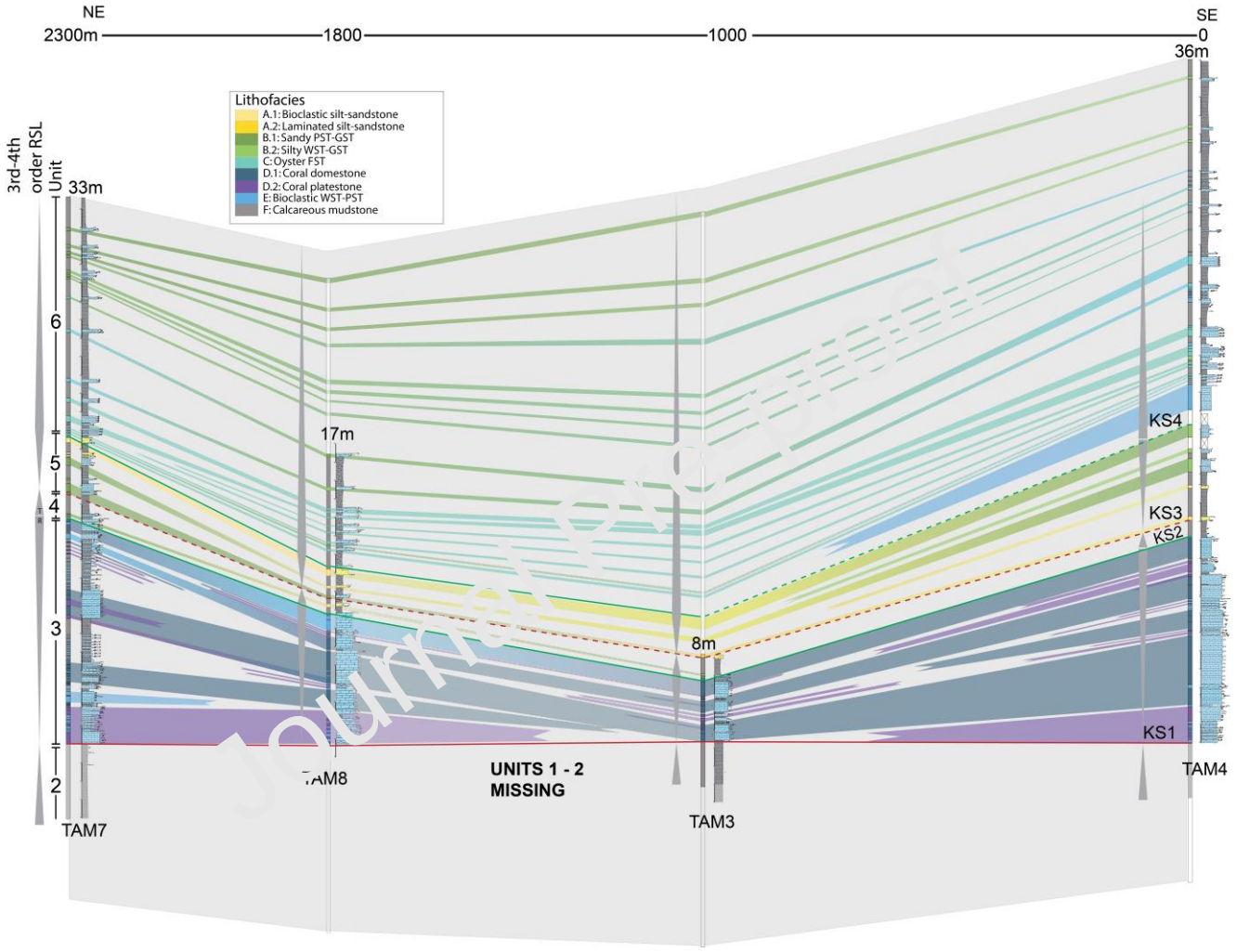

Figure 11 - Log Correlation Local northeast to southeast (line 2 on Fig. 1 Datum is the base of Unit 3 (KS1). Correlation of depositional sequences and sequence stratigraphic surfaces in an approximate strike direction in relation to the modern day coastline based on the logged sections in the Igourar location. Green line – transgressive surface, red line - regressive surface and dotted lines infer tentative correlation between sections. Geometric relationships are exaggerated (e.g. between TAM7-TAM8) most beds are horizontal to sub-horizontal in the field. Lighter shades for facies indicate inferred facies where there was lack of outcrop data due to modern fluvial erosion. 3rd to 4th order relative sea level cycles are also interpreted at each section.

4.4.2. Regional Correlation

The correlation was extended to the measured section AMS-1, 40 km to the north and an additional log south of the Cap Rhir anticline (Ain Hammouch section) modified from Bryers et al (2019) to build a regional framework for the Tamanar Fm. in the EAB. This allowed the construction of a regional north to south correlation to highlight the spatial and temporal distribution of units over tens of kilometres (Fig. 12).

Units 1 and 2 are not observed at the studied section south of the Amsittene anticline (AMS-1) nor are they seen on the southern side of the Cap Rhir anticline at Ain Hammouch (right side of fFig. 12). Unit 3 is found at all three logs along this 40 kilometre-length north-south transect, easily identified by the characteristic ferruginous, bioturbated and shell-encrusted hardground surface, KS2. The upward-thickening and then thinning trend of beds are a diagnostic feature of the unit that allows correlation between Igourar (TAM9), Ain Hammouch however it is not clear at AMS-1 whether the whole section has been deformed because of the late Mesozoic Atlasic Orogeny (Le Roy and Pique, 2001). Coral morphologies at Ain Hammouch are mainly thick-branching and surface-encrusting with only rare thin flat/platy morphologies present, concurrent with similar morphologies found at TAM9 and at AMS-1. Unit 4 can be correlated from Igourar to AMS-1 where it is thickest (6 m) and is made up of calcareous mudstones (lithofacies F) interbedded with poorly bedded bioclastic limestones (lithofacies E). The sand and silt-rich Unit 5 is recognised at AMS-1 but is thinner (from 15 at Igourar down to 3.5 metres at AMS-1). The individual beds are considerably thinner at AMS-1 than the other sections. In the south, at Ain Hammouch, the unit is slightly thicker (18 metres) and shows thickly bedded sandstones (50 cm to 2 m thick) with wavy and cross-laminations, rippled basal surfaces and relatively poor bioclast content. Above these the unit becomes more limestone-dominated but the beds retain their thickness. Unit 6 is thicker at Ain Hammouch (over 40 metres) with thicker beds of lithofacies C and E and more extensive calcareous mudstones interspersed between them. At AMS-1, the oyster-dominated limestones of Unit 6 are observed however the

aforementioned deformation has made detailed correlation impossible, and the true thickness has not been preserved.

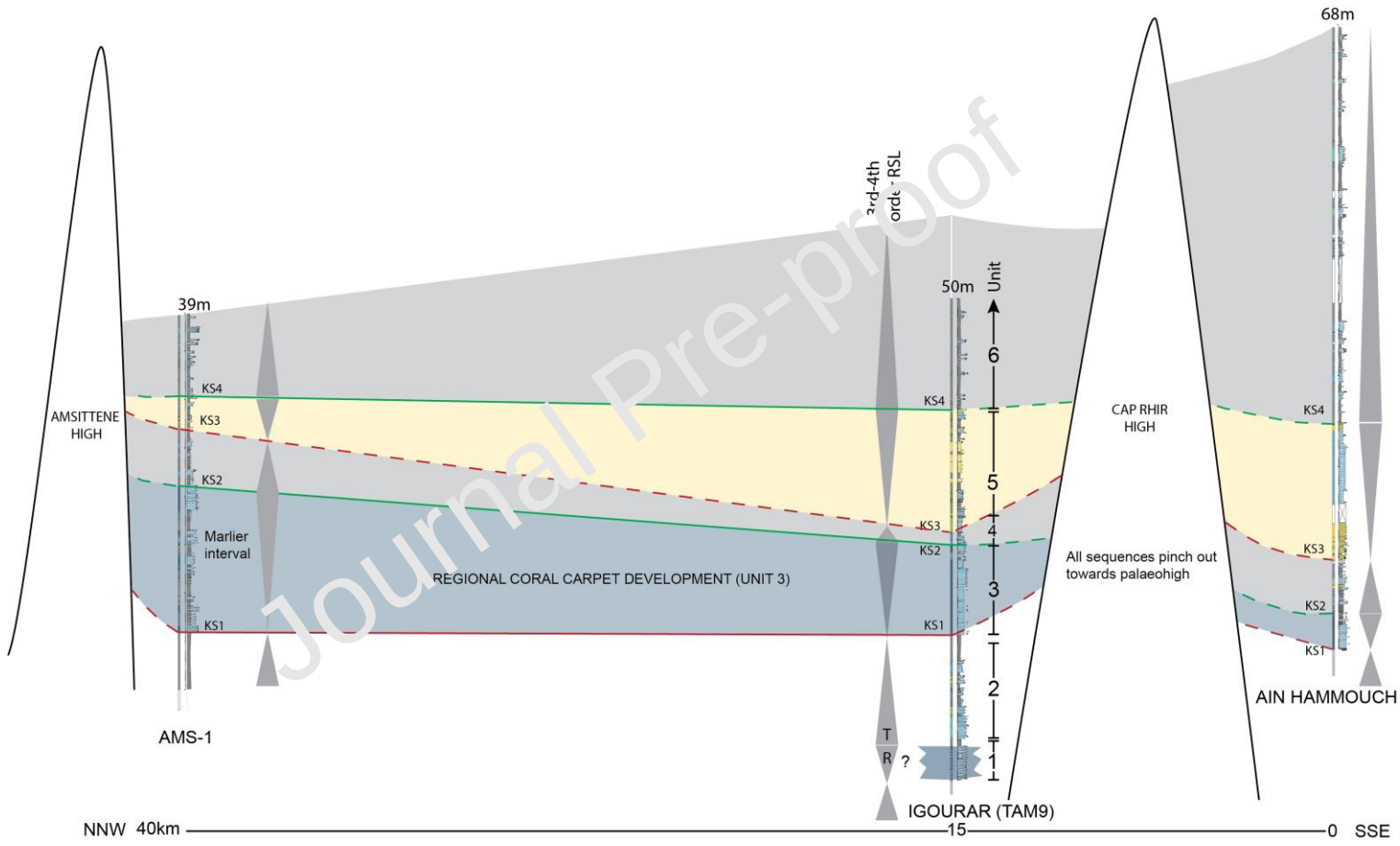

Figure 12 - Log Correlation Regional North to South (line 3 on Fig. 1). Regional log correlation between previously studied section Ain Hammouch (south of the Cap Rhir Anticline), TAM9 at Igourar (this study) and AMS-1, south of the Amsittene Anticline (an additional section logged during the field study).

5. Discussion

5.1. Depositional Evolution Model

The depositional evolution of the coral-rich Tamanar Fm. can be subdivided into six events. The depositional model (Fig. 13) utilises observations from both this study and previous field work on the margin and allowed identification of other sections that were found to contain corals in the Tamanar Formation (Ettachfini 2004; Ferry et al., 2007; Duval-Arnould., 2019). The presence of palaeohighs, illustrated in the accompanied diagrams, first reported in field studies by Luber et al., 2018 and Blanco et al., 2020, are also observed in this study and the correlated lower Cretaceous interval thins and then pinches out against these highs.

A - first colonisation of scleractinian corals in relatively shallow (15 - 30 m) and turbid water, marked by a sharp, undulating surface at the base of Unit 1. The corals are small and are made up of platy and delicate branching morphologies in a muddy matrix indicating low light/turbid conditions. The coral carpet growth is laterally very limited on the platform as the event is only identified at TAM9, suggesting fairly low platform productivity at this point in time. B - initial disappearance of the localised corals. Deposition was dominated by a series of bioclastic wackestone to packestones, oyster-rich floatstones and greenish-grey poorly bedded calcareous mudstones (Unit 2; lithofacies C, E and F) containing no corals. The facies shift is synonymous with declining water quality that prevented coral growth because of poor light quality/increased turbidity and relatively deeper water conditions. C - the bottom of Unit 3 is marked with a sharp base (KS1). This records the re-emergence of corals in the study area. The coral morphologies range from thick-branching phaceloid morphologies, undifferentiated domal shapes to thinner flat to platy-shaped morphologies all of which can vary in size. Their deposition is found across all the studied localities with similar assemblages and relatively equal thicknesses. An overall shallowing-up trend is observed in Unit 3: the upper part is dominated by thick-branching and dome-shaped corals indicating a shallower (5 to

15 m) inner platform whilst the lower beds typically bear flat/platy morphologies in a poorly lit slightly deeper middle platform (but no more than approximately 30 metres). The widespread, regionally recognised, growth of corals on the Morocco Atlantic margin suggests regional-to potentially global changes in palaeoenvironment and palaeoclimate that can be tied to time-equivalent coral growth and increased carbonate productivity relative to the underlying late Valanginian. D - A period of non-deposition occurs where coral growth plateaus, represented by a regionally correlatable marine hardground surface (KS2) suggesting very slow to zero sedimentation and increased water energy, at the top of Unit 3. Only surface-encrusting corals are seen and they are bio-eroded and usually heavily enriched in iron minerals. This marks a decrease in carbonate productivity on the platform. A thin interval of calcareous mudstones and limestones lies above KS2, representing the transgressive deposits that follow this surface. E - An irregular and sharp basal surface (KS3) marks a distinct increase in sub-angular to angular silt to fine sand sized clastic grains which can be sub-horizontally laminated and have sharp-based beds with a relatively reduced bioclastic content. These are interpreted as a shoreface depositional environment and no corals are observed. This event can be correlated with an increase in humidity that led to greater terrestrial runoff and associated siliciclastics and is documented across the Tethys (Arias et al., 1995; Föllmi et al., 2007). F - Marked by KS4, which proceeds several beds with shell debris concentrations (mainly oysters) at their bases (top of Unit 5) marking the retreat of the shoreface (e.g. section TAM9 at the top of Unit 5 in Fig. 10). KS4 is proceeded by a series of oyster floatstones with oysters up to 10 cm diameter) that dominate the faunal assemblage and are followed by upward-thickening calcareous mudstones and occasional limestones containing ammonites and nautiloids which suggest a deepening trend and relatively unproductive outer platform conditions.

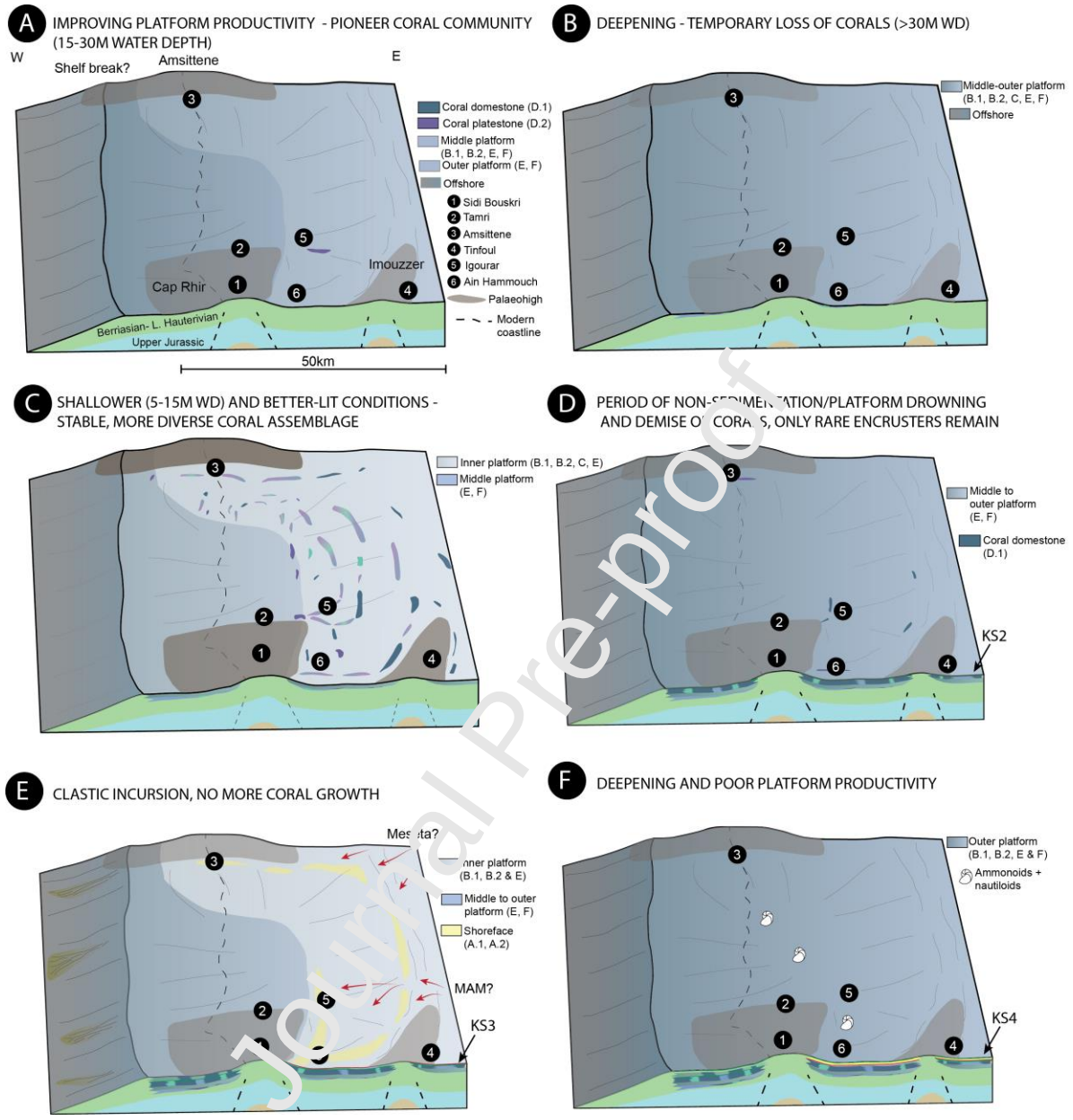

Figure 13 - Depositional Models Mosaic (6 models). 3-dimensional concept models for the series of depositional sequences interpreted. Location 4 (Tinfoul) shows the most easterly occurrence of corals on the margin. True fluvial facies are not observed onshore the EAB, however red silts of late Hauterivian age are found near the settlement of Imintanoute. The red arrows in part E show potential sediment input from known continental highs that may have been exhumed during the earliest Cretaceous. The position of the shelf break is inferred from Tari and Jabour (2013). A – relative sea level fall following a transgression during the late Valanginian allows limited coral establishment (made up of small platy and thin-branching morphologies. B – A 3rd order sea level rise makes water depth too great for corals (approximately > 30 m). C – Corals are widespread along the margin with a relative sea level fall (water depths approx. 5-15m) and related improving environmental conditions. Domal and thick-branching morphologies dominate however to the west at Igourar the platy morphologies become preferred with a gentle deepening of the platform. Corals change preferential shape from larger domal shapes and thick-branching shapes to flat/platy ones over short distances independent of this basinward deepening, attributed to local environmental factors affecting turbidity. D – A regionally correlatable break in sedimentation followed by a short transgression ends coral development in Morocco, only resilient surface encrusters are observed on the hardground surface (KS2). E – A shoreface environment develops with the progradation of elongate silt to fine sands. F – A transgression leads to outer platform conditions across the margin and poor productivity is evident by depauperate oyster

communities. These oyster floatstones were deposited during episodic storm events between predominantly calcareous mudstone deposition.

5.2. Establishment of coral carpets

In the EAB, thin ammonite-bearing limestones and greyish-green calcareous mudstones underlie the Tamanar Formation, interpreted as recording outer platform conditions. The macrofossil content decreases whilst the silt content increases upwards, pointing to unfavourable platform conditions that may be related to cooler ocean waters evidenced in the mid to upper Valanginian positive δ13C isotope excursion Weissert Event (Erba et al., 2004; McArthur et al., 2007). The emergence of coral-bearing beds lying abruptly on top of these silt-rich and fossil-poor calcareous mudstones and limestones points to a recovery of the health of the carbonate platform. The initial establishment of corals in the studied interval is by small flat/platy and delicate-branching forms in a muddy matrix (Unit 1). This was the pioneer species that temporally established prior to the increase in distribution, abundance and relative diversification of morphologies identified in Unit 3. Similar ecological succession has been observed in the older Oxfordian reefs in SW Morocco (Olivier et al., 2012; Duval-Arnould, 2019) and in the Northern French Jura (Lathuilière et al., 2005).

The widespread development of corals (Unit 3) on the western Moroccan Atlantic margin and the numerous documentations of the emergence of time-equivalent (Hauterivian-aged) coral deposits worldwide for example in SE Spain (Arias et al., 1995; Löser., 2008), SE France (Masse et al., 2009) and the Neuquen basin in Argentina (Garberoglio et al., 2013) suggest global-scale palaeo-environmental changes. McArthur et al. (2007) suggest warming Tethyan seas from the late Valanginian to early Hauterivian in the SE Mediterranean, van de Schootbrugge et al. (2002) indicate increasing ocean temperatures in the Tethyan and Boreal realms from the *Radiatus* to C. *loryi* ammonite zones. Furthermore, a recent review by Scotese et al. (2021) suggests a global increase in ocean temperatures between the late Valanginian to early Hauterivian.

On the northern Tethyan margin, faunal evidence points to heterozoan-rich communities during the lower Hauterivian (Föllmi et al., 2007) which is thought to be linked with detrital influxes

from the continent. Corals (of both lithofacies D.1 and D.2) shared habitats with heterozoan-rich communities in the EAB (e.g. oysters, bryozoans, serpulids, brachiopods and echinoderms) and both lithofacies show varying quantities of quartz in the matrix and preserved in the individual corallites post-mortem. This suggests a broad relationship across the Palaeotethys, where nutrient-rich environments associated with increased terrugenous material shedding from continental areas were common on shallow marine platforms. The low-diversity and widely spaced corals, independent of morphology, in Units 1 and 3 (illustrated in Fig. 4) were most likely opportunistic in a mesotrophic environment. The micro-encruster *Lithocodium Aggregatum* commonly associated with the corals is not observed in the underlying (Berriasian to Valanginian) deposits in the EAB, which also supports changing environmental conditions, and perhaps increasing nutrient levels. Increasing nutrient levels associated with higher detrital input was similarly suggested as a factor for *Lithocodium-bacinella* blooms during the Aptian in Oman (Rameil et al., 2010).

The early Hauterivian is set in a period of long-term, global relative sea-level rise, of over tens of millions of years (Fig. 2; Haq., 2014; Simmons et al., 2020). However, on a shorter time-scale (several millions of years), a relative sea-level lowstand is suggested during the late(est) Valanginian and earliest Hauterivian in south-western Morocco (Rey et al., 1988) and in the Mediterranean Tethyan realm (McArthur et al., 2007). The gross depositional stacking patterns indicate an overall shallowing up from Units 1 to 5 that is correlated locally at Igourar (Fig. 10 and Fig. 11) and regionally over tens of kilometres (Fig. 12) pointing to a regional eustatic control on deposition. This is illustrated by the change from smaller platy and thin-branching forms in Unit 1 to large thick-branching and dome-shaped corals within thicker beds in Unit 2 and culminates with the shoreface silts and sandstones that are observed in Unit 4.

The inherited platform morphology also played an important role in the development of coral carpets. The underlying series of limestones and calcareous mudstones of Berriasian to late Valanginian age are generally flat to slightly undulating in nature (Bryers et al., 2019) and show

similar planar geometries to the Tamanar Formation. The flat and relatively uniform platform promoted laterally extensive but vertically limited coral growth, with no reef frameworks identified at the studied outcrops. Modern examples of non-framework reefs from the Red Sea (Riegl and Piller; 1997, 2000) and the Gulf of Aden in Yemen (Benzoni et al., 2003) indicate the initiation of low relief coral carpet communities is linked to relatively flat seafloor topographies.

Early marine diagenesis is prevalent throughout the studied sections. Shallow, well-agitated waters in calcite-precipitating seas during the early Cretaceous (Sandberg, 1983) combined with the wide and gentle platform morphology and low-sedimentation rates promoted early marine cementation of the seafloor. In the study area, this is evident from the widespread microspar and blocky calcite in skeletal fragments, including the coral structures (Fig. 6). Microbial activity evident from the abundant *Lithocodium Aggregatum* and coralline red algae *Sporalithon Rude* could have further enhanced the strength of individual colonies and allowed them to survive relatively high water energy and episodic storms. This was more important for the thick-branching and massive forms (D.1) than the flat/platy forms (D.2), which relied on a hard-substrate in their higher energy environment.

Therefore, a combination of changing palaeo-environmental conditions, relative sea level fall, and an aerially-extensive low-relief platform, facilitated coral carpet development in the early Hauterivian age in SW Morocco.

5.3. Controls on coral morphology, abundance and distribution

The biostratigraphic constraint provided by the ammonoids collected (see *Biostratigraphy* section, Fig. S2) suggests the coral-bearing interval of units 1 to 3 were deposited within the *Crioceratites loryi* zone of the lower Hauterivian; a period spanning approximately 500 to 600 kyr (Reboulet et al., 2018; Gale et al., 2020). If the thickness of coral-bearing units 1 to 3 at TAM9 is 25 metres, this would mean each metre of section would amount to approximately 20 to 24 kya. This is concordant with minor amplitude sea level changes in the Hauterivian (Ray et al., 2019). Fauna (such

as oysters, echinoderms, serpulids) and infaunal benthic foraminifera (dominated by texturaliids such as *Praedorothia* sp.) and the common micro-encrusting *Lithocodium Aggregatum* that is associated with shallower water (Schmid and Leinfelder., 1996) are observed in both D.1 and D.2, but they have a greater depth range than the more environmentally-sensitive corals, so high frequency sea level fluctuations of several tens of metres over tens of thousands of years could be plausible as a control on temporal variations in coral morphology. However, given that the platform appears to lack topographic irregularity, and only steepens very gently to the west over several kilometres (the transition to platy-dominated beyond TAM2 and total loss of corals beyond TAM5), significant bathymetric changes over hundreds of metres seem unlikely to account for local-scale morphological changes or other facies variations identified laterally.

Light levels, hydrodynamic energy, sedimentation and turbidity are key drivers in shaping coral communities (Hallock and Schlager, 1986; Rosen et al., 2000; Dupraz and Strasser, 2002; Sanders et al., 2005) and their interplay is significant in coral morphology, abundance and distribution in time and space in the EAB. Platy corals (Microsolenid subgenus) in the nodular-bedded typically wackestone matrix indicate an adaptation to poorer light conditions (Insalaco et al., 1996; Kolodziej et al., 2020) whereas larger densely packed thick-branched and massive dome-shaped corals in a typically packstone matrix record a morphological response to increased light/ higher energy environments (illustrated in Fig. 14). Similar responses to changes in light levels have been documented in Aptian-aged scleractinian corals from the Maestrat basin (Tomas and Löser., 2008; Arnal et al., 2012); platy corals were interpreted as an adaptation to poorly lit outer shelf settings and domal-shaped corals were attributed to shallower and higher energy inner ramp settings (depths up to 30 metres in both cases). In both lithofacies in Morocco, mud (usually micritised) quantities are high in both the matrix and within coral remains and other bioclasts suggesting turbidity was relatively high (although greater in platy coral-rich D.2) and factored into the development of widely-spaced, low-diversity and isolated coral communities.

Lateral shifts between coral morphologies and shifts from non-coral to coral-bearing deposits, could occur without clear bathymetric shifts as many fauna and flora are found in different lithofacies. This suggests that these spatial changes are related to differing environmental conditions affecting sediment input. Autogenic controls (independent of processes such as tectonics, climate and relative sea level) that affect sedimentation and erosion are key drivers for local (tens to hundreds of metres) lateral facies variability in modern and ancient shallow marine systems (Schlager, 2003; Wright and Burgess., 2005; Purkis and Harris., 2016 and Moscardelli and Wood., 2019; McNeil et al., 2020). The lateral changes in morphology and presence or absence of corals is variable between logged sections on a scale of hundreds of metres, which suggest similar environmental factors, sedimentation and erosion (i.e. changes in hydrodynamic regime), had a direct influence on coral communities. Changing terrestrial runoff (Hallock and Schlager, 1986), variable currents, tidal regimes and/or episodic storm action effect the balance of erosion and sedimentation and therefore turbidity (Sanders et al., 2005; Westphal et al., 2010). The platy, branching and domal corals indicate adaptations to varying hydrodynamic energy and turbidity (as illustrated in Fig. 14). For example, dorval shapes or thickets of large, phaceloid-branching corals (with individual corallites up to two centimetres in diameter) suggest adaptation to increasing water energy, whereas the smaller and thinner morphologies may reflect quieter and more turbid conditions resulting in poorer light levels (Dupraz and Strasser, 2002; Ricci et al., 2018).

The low relief and relatively uniform geometry of the platform may have allowed swift migration of sediment bodies and erosive processes to occur with changeable currents and/or changes in terrugenous input. Similar processes would explain shifts in lithofacies in the non-coral bearing units for example from A.1 or A.2 to B.1 or B.2 between sections TAM7 AND TAM8 in Unit 5 (approximately 700 metres).

Substrate availability is influenced by sedimentation type, rate and water energy (Westphal et al., 2010) which could partly account for the scattered and apparently unsystematic coral

abundance. The position of the flat/platy corals (D.2) in a muddy matrix and the bio-erosion at their highly irregular basal surfaces suggest they did not rely on a hard substrate like the larger corals (Fig. 14). The thick-branching and undifferentiated massive morphologies (D.1) convey non-planar cemented surfaces at their bases suggesting a hard substrate was necessary for their colonisation. Changing substrate from areas of hard seafloor to areas of soft muddy sediment therefore contributed to the coral morphology.

The high abundance of heterotrophs found in the coral-rich Units 1 and 3 (bio-eroding echinoderms and various filter feeding such as oysters and bryozoans) could also have limited coral growth and increased spatial heterogeneities through increased predation, grazing and natural competition for nutrients and substrate space (Schlager, 2003; Wright and Burgess, 2005; McNeil et al., 2020). Analogous examples are found in the Middle Miocene in Austria (Riegl and Piller, 2000) where facies vary over tens of metres in short (less than one-metre-thick) coral carpet framework and non-framework communities are observed across a low-relief platform and are interpreted to be strongly influenced by the hydrodynamic regime and sedimentation. Modern day examples found in the modern Red Sea (Riegl and Piller, 1997, 2000) also show similar autogenic controls on the coral morphology and distribution. This random component of shallow carbonate sedimentation is difficult to evidence in the ancient record but it is nevertheless likely that it interfered with the high-frequency relative sea level cycles and gave rise to facies variations and varying coral morphologies.

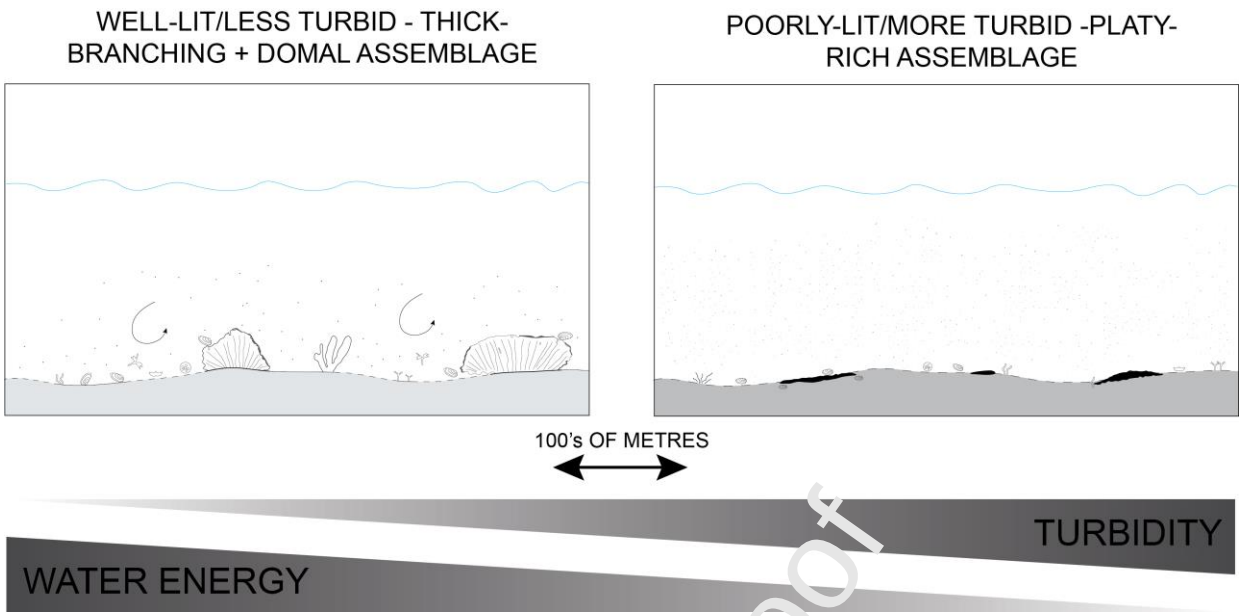

Figure 14 –Simple conceptual model for changing coral communities with changing environmental conditions (a factor of light level related to turbidity and hydrodynamism). Water depth is constant, varying shades of grey indicate seafloor sediment (darker grey is muddier). Hard substrate is shown as a hard black line and softer substrate is shown as a dotted black line. At higher turbidity the light level is reduced and corals grow preferentially in flatter to platy morphologies. At higher hydrodynamic levels and lower turbidity (i.e. better lit environments), the corals show a preference for thick-branching and massive forms. Sedimentation rate is interpreted as low overall. For this change to occur, local-scale environmental conditions shift, for example from a less sheltered to more sheltered environment where finer sediments (e.g. mud particles and/or silts) accumulate. This model excludes the gradual deepening that is observed at Igourar from east to west resulting in platy corals replacing thick-branching and domal forms before completely disappearing and also the temporal shifts from D.1 to D.2 (inner to middle platform) interpreted as deepening events.

5.4 Coral Demise

The ferruginous, irregular and shell-encrusted surface (KS2) marking the end of coral growth at the top of Unit 3 is interpreted as a drowning surface, where rapid sea level rise resulted in a reduction or complete shutdown of carbonate production (Kendall and Schlager, 1981; Godet et al., 2013). A similar ferruginous and non-planar surface has been reported at a similar time interval capping Lower Hauterivian coral development in SE Spain (Arias et al., 1985). The transgressive surfaces may be associated with Tethyan-wide palaeoenvironmental change, such as those reported in the Helvetic platform where drowning unconformities constrained to the *C. loryi* ammonite zone of the early Hauterivian (Föllmi et al., 2007) are partly linked with increasing humidity and the associated detrital influx resulting in a lowering productivity of the carbonate platform. A longstanding sedimentary hiatus, correlated over tens of kilometres in the EAB, could have subjected the platform to erosive wave-action, storms and deeper water which would have led to the end of coral development. The relatively short-lived 3rd to 4th order deepening (Unit 4) that

proceeded KS2 led to limited substrate availability and unfavourable carbonate productivity that further deteriorated with the subsequent progradation of shoreface clastics (Unit 5). Corals are not observed as whole or as debris in Unit 5 at an outcrop or microscopic level suggesting coral growth had completely ceased prior to the increased and sustained clastic supply. They could not re-establish after the drowning event with the reduction of hard substrate availability for colonisation and given the low seafloor relief the efficiency of sediment rejection may have been made more difficult than on inclined or declined slopes where sediment would be less likely to accumulate (Dupraz and Strasser, 2002; Sanders et al., 2005). In SE Spain, the lower Hauterivian also contains corals, interpreted as shallow water bioherms, draped by cross-bedded calcareous sandstones (Arias et al., 1995) which supports the idea of increasing humidity resultant in hinterland erosion and clastic input on carbonate platforms on a greater scale.

Decreasing carbonate platform health culminated with the deepening recorded in Unit 6 and the deposition of depauperate oyster beds. The oysters are large and make up the majority of the faunal assemblage, suggesting they were able to withstand environmental conditions that other fauna could not. Platform demise, dated as late early to early late Hauterivian, on the northern Tethyan margin (Föllmi et al., 2007) represented by glauconite and phosphate-rich limestones beds are roughly time-equivalent to the oyster-dominated succession documented in the EAB. Given that the drowning surface marking the end of coral growth is correlatable over tens of kilometres in SW Morocco, it would seem likely this was a regional event related to unfavourable palaeoenvironmental conditions associated with an initial deepening on the platform followed by the progradation of shoreface clastics.

6. Conclusions

The coral-rich carpets of the Tamanar Formation have been characterised and the controls examined through integrating sedimentology, mapping and facies analysis, and the following key points can be deduced:

- Two coral-rich units are identified; a lower, isolated horizon, 4 m in thickness and an upper horizon between 5 to 15 metres thick that extends for several thousands of metres. They are made up of sparsely distributed scleractinian coral communities that co-existed with a heterozoan-rich faunal assemblage with variable amounts of siliciclastics forming planar low-relief carpets with no internal zonation or reefal build-up geometries.
- The Tamanar Formation can be dated to have been deposited within the *C. loryi* auct. ammonite zone, suggesting an approximate timespan of 500 to 800 kyr.
- Favourable growth conditions for corals arose with changing palaeoenvironmental conditions and 3rd order relative sea level fall that lead to a more productive carbonate platform than in the preceding Valanginian age.
- The low-relief antecedent seafloor of the earliest Cretaceous platform influenced coral development, favouring non-framework carpet geometries rather than framework reef build-ups and permitted wave-agitation that resulted in widespread early marine cementation of individual corals.
- The two coral lithofacies – domestones (thick-branching phaceloid and undifferentiated massive forms in a bioclastic matrix) and platestones (thinner flat/platy forms in a muddier matrix) temporally reflect low-amplitude high-frequency relative sea level fluctuations. The platy/lenticular-shaped coral beds indicate lower energy/turbid settings in slightly deeper platform conditions than the thick-branched and massive-shaped coral dominated beds that developed in the higher energy, better-lit, shallower platform environment. However local-scale coral morphology and lateral facies changes are interpreted to be linked to autogenic factors, independent of bathymetric change which were most importantly shifts in turbidity and water energy laterally.
- The termination of coral growth is marked by a regionally correlatable hardground representing a drowning event and deteriorating platform health. This was quickly

followed by an influx of silt to fine sized siliciclastics and then depauperate oyster communities and silt-rich calcareous mudstones. This represents a temporal palaeoenvironmental change with increasingly poor platform health and is recognised across the Tethyan realm and associated with an increasingly humid climate and a related influx of terrugenous material.

- These outcrops in western Morocco allow a key contribution to the relatively sparse documentation of Hauterivian corals. Their sparse abundance, preference of lateral growth and poor diversity is mirrored in time-equivalent coral-bearing sections around the globe, suggesting a that corals where opportunistic and grew in recovering and/or mesotrophic carbonate platforms.
- These low-diversity and sparely distributed corals from a greenhouse period may provide a proxy for recovery and demise of corals in response to environmental stress to both modern and future climate change projections.

Acknowledgements

The work has been carried out as part of a PhD study fully supported by the North Africa Research Group (NARG) at the University of Manchester. The authors would like to thank Stefan Schroeder and Max Cassou for their help in the synthesis of this paper.

Appendix – Supplementary data

Associated supplementary data can be accessed on the online version: >URL<

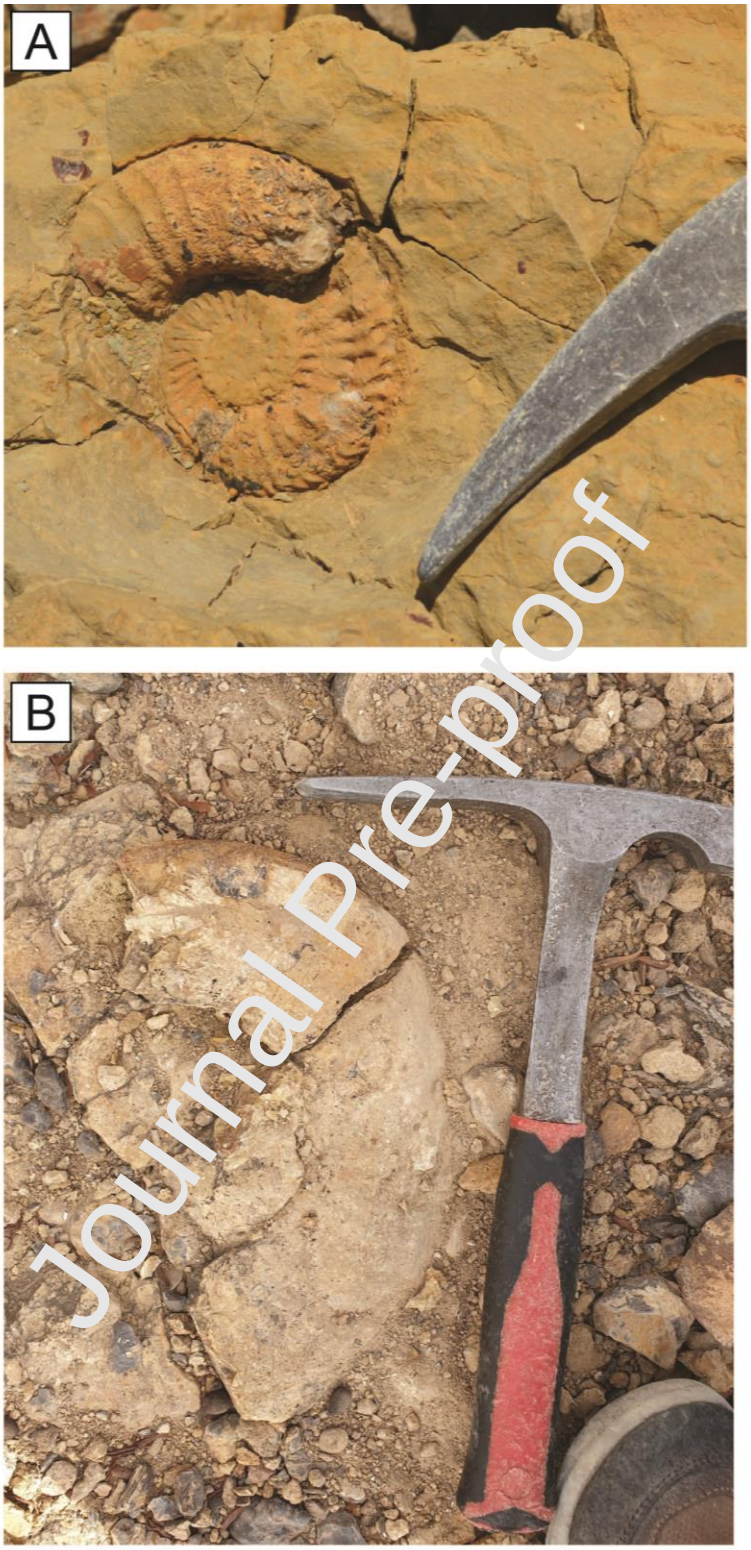

Figure S1 – Ammonites found in the field. A – Newly established ammonite genus Haroella, this paper does not discuss the new genus. B – Lyticoceras gr. *Cryptoceras. Hammer head width 15 cm.*

Thin Section ID	Diagenetic Overprint	Skeletal Remains	Skeletal Remains (%)	Micritic Content (%)	Visible Porosity (%)	Quartz Content (%)
TAM8 47S	Blocky calcite and microsparite v common, rare fibrous	Echinoids (v common), forams, bryozoan, coral	60	30	5	5

		frag (scleractinian?), oyster or other bivalve frag (fibrous)				
TAM3 51S	Blocky and horizontal calcite and fibrous within bivalvia remains	Echinoids v common, oysters, large branch-like remains filled with micrite could be coral frag?	50	50	0	5
TAM7 53S	Fibrous and blocky calcite in remains	Bryozoan, echinoids, oyster?	30	20	2	50
TAM9 41S	Rare, sparse irregular calcite in remains	Common elongate shell fragments (oysters, bivalves?	20	20	0	60
TAM4 48S	Skeletal remains can have semi-fibrous or blocky calcite	Bryozoans common, elongate shell frags (oysters), echinoid frags	30	0	0	20
TAM1 45C	Blocky calcite dominates with horizontal and syntaxial (twin lamallae) also common	Unclear due to cementation	80	18	2	0
TAM4 47C	Blocky common within remains, also some fibrous and matrix commonly with microsparite	Oysters, echinoids, forams, Lithocodium Aggregatum, coralline red algae	50	40	0	10
TAM8 46C (B)	Dominated by blocky calcite, rare microsparite.	Mostly cemented and few clear skeletal remains preserved although several large shell outlines	85	15	0	0
TAM4 46S	Blocky calcite common and significant microsparite content, rare fibrous/bladed in remains	Large coral fragments, bryozoans. Echinoids, small forams, many undiff' remains	45	40	10	5
TAM10 42C	Dominated by blocky calcite, rare microsparite. Within crystals horizontal layers in cements	Unclear due to cementation	80	20	0	0
TAM2 57S	Small rhomboidal (dolomite or microsparite?) crystals with more common blocky calcite	Oysters, coral pieces and echinoids, Lithocodium Aggregatum	60	30	5	5
TAM9 52S	Highly crystalline with blocky calcite and in places	Few crystallised shell remains	30	20	0	50

	rhomboidal (dolomite?)					
TAM8 44S	Calcite within skeletal remains	Oysters, bryozoan, Lithocodium Aggregatum	50	43	2	5
TAM1 52S	Calcite blocky and fibrous in skeletal remains	Oysters, coral fragments, bryozoan, echinoids	30	60	5	5
TAM9 47S	Generally blocky calcite fills skeletal remains	Echinoids v common, gastropods (or small foram?)	45	50	0	5
TAM2 58C	Dominated by blocky calcite (80%)	Unidentifiable due to recrystallization of calcite	N/A	10	1	0
TAM9 40C	Blocky and some fibrous cements of remains	Variable sized, crinoids(or serpulids?) common, possible oyster boring filled with micrite, outline of larger coral piece?	30	60	0	10
TAM8 40C	Blocky and fibrous calcite common	Oysters, echinoids, bivalves(?), serpulids, gastropod (or foram?)	39	50	1	10
TAM7 44C	Some blocky and fibrous cement	Echinoids (or coral?), oysters and/or brachs, serpulids and an encrustation possibly from an oyster, crinoid(?), small gastropod (or foram?), Lithocodium Aggregatum	48	40	2	10
TAM4 40C	Blocky calcite common	Bivalves (oyster?), elongate fragments crystallised, echinoids	40	44	1	15
TAM3 54C	Large to small blocky calcite, also fibrous to bladed in several remains	Bryozoan (v common), gastropod, echinoid, large elongate shell fragments, brachiopod, bivalve, serpulid, corals	50	30	0	20
TAM8 44BC	Almost completely calcite recrystallized. Large blocky to more fibrous or sinuous	Only coral branch outlines visible in macro view	80	20	0	0

TAM9 42S	Only sparse calcite cementation of small skeletal remains, perhaps microsparite in them too. Some fibrous cement in elongate remains	Bryozoan, bivalve, echinoid, serpulids, numerous elongate fragments (oysters?)	30	30	0	40
TAM2 61S	Very commonly fibrous in shell remains and some blocky calcite,	Oysters, brachiopods, echinoids, variable sized remains	40	20	0	40
TAM4 41C	Totally recrystallized by calcite, mainly blocky but some more fibrous	Undeterminable but likely recrystallized coralites	90	10	0	0
TAM3 53C	Recrystallized by blocky calcite of variable sized crystal	Undeterminable but likely recrystallized coralites	90	10	0	0
TAM6 41C	Large blocky calcite with lamellae clear within crystals. Also smaller blocky calcite common and microsparite. Rare fibrous	Bryozoans, one encrusting coral fragment, coral fragments large and have microbial encrustations, lots of tiny circular remains, few fibrous shell fragments, coralline red algae	50	35		15
TAM7 47C	Blocky calcite, can be twinned. Fibrous common in shell fragments, rare bladed in remain	Echinoid, large oysters, tiny skeletal remains (peloids, forams?)	50	40		10
TAM4 44S	Common blocky calcite, some twinning lamallae. Some fibrous to bladed cements	Bivalves, bryozoan, serpulid, echinoid, brachiopod, Lithocodium Aggregatum	45	45		10
TAM2 53C	Largely recrystallized by blocky calcite, variable sizes. Rare bladed to fibrous in shell remains. Microsparite common	Large algal? fragments, many small shell fragments and some larger elongate (oyster, brachiopod?)	60	34	1	5
TAM9 50C	Almost entirely recrystallized by small blocky calcite, some with lamellae, also common microsparite	Coral outlines only visible, likely recrystallized coralites	90	10	0	0
TAM7 49C	Some blocky calcite within large coral fragments, common v. fine crystals, microsparite? Some fibrous calcite skeletal remains	Corals, many small and elongated remains, echinoid	40	50	0	10

TAM10 41S	Dominated by variable sized calcite crystals, mainly blocky. Microsparite in coral fragments. Some twinning of calcite	Corals	60	30	0	10
TAM10 40C	Recrystallised calcite of variable blocky style, some twinning.	Corallites recrystallized by calcite	90	10	0	0
TAM6 43C	Variable calcite cementation, blocky, some syntaxial cement, some fibrous to bladed in remains	Large recrystallized coral pieces, Echinoids (v. common), serpulids, crinoid(?), bryozoans, forams	40	50	0	10
TAM4 42C	Blocky calcite common, variable size, some horizontal lamellae, fibrous calcite common in remains	Large coral branch pieces, many bryozoan fragments, echinoids, shell pieces (could be bivalves, brach or oysters or mix), Lithocodium Aggregatum	50	40	0	10
TAM5 42S	Very fine blocky calcite, common fibrous, and syntaxial cements in remains, microsparite also common	Stromatoporoid, bryozoans, serpulids, echinoids, oysters and other elongate fibrous-cemented fragments, forams with agglutinated quartz internally, coral fragment(?),	60	20	2	18
TAM7 52S	Fine blocky calcite to micosparite, fibrous cementation of elongate remains common	Bryozoans, serpulids, belemnite(?), echinoids, elongate shell fragments very common	55	39	1	5
TAM9 50B S	Fine blocky calcite, microsparite common also between remains	Mainly bryozoans and echinoids, possible coral flower remains (micrite filled)	40	39	1	20
AMS1 70S	V. common calcite as blocky both fine and large sizes, also commonly twinned and may be fibrous when part of shell fragments. Microsparite common	Corals, echinoids, oysters, bryozoan fragment(?) and elongate shell fragments	50	40	0	10

TAM7 41C	Blocky common, fibrous also, some twinning lamellae. Very fine calcite crystals to microsparite common in matrix	Bryozoan, elongate shell frag (oyster?), small dark dots maybe forams	40	40	0	20
TAM6 47S	Fibrous and microspar in skeletal remains	Echinoids, serpulids, oysters, bivalves	25	30	5	40
TAM5 40S	Blocky and fibrous, some twinned in large skeletal remains	Large remains of echinoids, shelly fauna, bryozoan, serpulids	29	40	1	30
TAM7 43S	Very clear blocky, fibrous and rhomboidal (still calcite?) calcite and some twinning. One large fragment with outer part showing bladed cement	Large fragments, serpulids, bryozoans, echinoids, oysters, coralline red algae	30	40	15	15
TAM2 54S	Common in skeletal remains, serpulids have outer fibrous cement in places. Blocky and fibrous.	Echinoids, oysters, serpulids, bryozoans, possible coral frags	35	35	15	15

Table S1 - Microfacies sheet produced during thin section analysis of samples. Percentages are based on estimates from thin section optical view)

References

Aguirre-Urreta, M.B., Price, G.D., Ruffell, A.H., Lazo, D.G., Kalin, R.M., Ogle, N. and Rawson, P.F. (2007) Southern Hemisphere Early Cretaceous (Valanginian-Early Barremian) carbon and oxygen isotope curves from the Neuquén Basin, Argentina. Cretaceous Research (29), 87-99.

Ambroggi, R., 1963. Etude géologique du versant méridional du Haut-Atlas occidental et de la plaine du Souss. Notes et Mémoires du Service Géologique du Maroc 157, 1–322.

Arias, C., Masse, J.P and Vilas, L. (1995) Hauterivian shallow marine calcareous biogenic mounds: S.E. Spain. Palaeogeography, Palaeoclimatology, Palaeoecology (119), 3-17.

Bover-Arnal, T., Salas, R., Martin-Closas, C., Schlagintweit, F and Moreno-Bedmar, A.J. (2011) Expression of an oceanic anoxic event in a neritic setting: lower Aptian coral rubble deposits from the western Maestrat Basin (Iberian Chain, Spain). Palaios (26), 18-32.

Benzoni, F., Bianchi, C.N. and Morri, C. (2003) Coral communities of the northwestern Gulf of Aden (Yemen): variation in framework building related to environmental factors and biotic conditions. Coral Reefs (22), 475-484.

Bromley, R.G. and Asgaard, U. (1991) Ichnofacies: a mixture of taphofacies and biofacies. Lethaia (24), 153-163.

Bryers, O., Bulot., L., Redfern, J., Casson, M., Ettachfini, M., Masrour, M, Rehakova, D and Jeremiah, J. (2019) Establishing a high resolution integrated stratigraphic framework for the Berriasian to early Barremian of the Morocco Atlantic Margin. In: PESGB-HGS Africa E&P Conference, October 2019, London.

Bugrova, I.J. (1990) The facies zonation and scleractinians of the early Hauterivian reef complex of Bolshoy Balkhan. Cretaceous Research (11), 119-230.

Bulot, L.G., Thieuloy, J.P., Blanc, E and Klein, J. (1992) Le cadre stratigraphique du Valanginien supérieur et de l'Hauterivien du Sud-Est de la France: définition des biochronozones et caractérisation de nouveaux biohorizons. Gé

ologie Alpine (68), 13-56.

Busnardo, R and Thieuloy, J.P. (1989) Les ammonites de l'Hauterivien jurassien: révision des faunes de la région du stratotype historique de l'étage hauterivien. Mémoire de la Société neuchâteloise de. Sciences naturelles (11), 101–147.

Butt, A. (1982) Micropaleontological bathymetry of the Cretaceous of western Morocco. Palaeogeography, Palaeoclimatology, Palaeoecology (37), 235–275.

Carson, G.A and Crowley, S.F. (1992) The glauconite-phosphate association in hardgrounds: examples from the Cenomanian of Devon, southwest England. Cretaceous Research (14), 69-89.

Catuneanu, O., Galloway., W.E., Kendall, C.G.St.C., Miall, A.D., Posamentier, H.W., Strasser, A and Tucker, M.E. (2011) Sequence Stratigraphy: Methodology and Nomenclature. Newsletters on Stratigraphy (44), 173-245.

Charton, R., Bertotti, G., Duval-Arnould, A., Redfern, J and Storms, J.E.A. (2020) Low-temperature thermochronology as a control on vertical movements for semi-quantitative source-to-sink analysis: A case study for the Permian to Neogene of Morocco and surroundings. Basin Research (#?).

Charton, R., Kluge, C., Blanco, D.F., Duval-Arnould, A., Bryers, O, Redfern, J and Bertotti, G. (2021) Syn-depositional Mesozoic siliciclastic pathways on the Moroccan Atlantic margin linked to evaporite mobilisation. Marine and Petroleum Geology (128).

Cherchi, A and Schroeder, R. (2013) Revision of the holotype of Lithocodium aggregatum Elliott, 1956 (Lower Cretaceous, Iraq): new interpretation as sponge–calcimicrobe consortium. Facies (59), 49–57.

Christ, N., Immenhauser, A., Wood, R.A., Darwich, K and Niedermayr, A. (2015) Petrography and environmental controls on the formation of Phanerozoic marine carbonate hardgrounds. Earth Science Reviews (151), 176-226.

Cotillon, P. and Rio, M. (1984) Cyclic sedimentation in the Cretaceous of Deep Sea Drilling Project sites 535 and 540 (Gulf of Mexico), 534 (central Atlantic), and in the Vocontian Basin (France). Init. Rep. Deep Sea Drilling Proj. (77), 339–376.

Davison, I. (2005) Central Atlantic margin basins of North West Africa: Geology and hydrocarbon potential (Morocco to Guinea). Journal of African Earth Sciences (43), 254–274.

Duffaud, F., Brun, L., Planchut, B. (1966) Le bassin du Sud-Ouest marocain. In: Reyre, D. (Ed.), Bassins sédimentaires du Littoral africain, Symposium de l'Association des Services géologiques africains (New Dehli, 1964), 1ère partie, Littoral Atlantique, 5–12. Firmin Didot Publications, Paris.Dunham 1962.

Dupraz, C and Strasser, A. (2002) Nutritional Modes in Coral: Microbialite Reefs (Jurassic, Oxfordian, Switzerland): Evolution of Trophic Structure as a Response to Environmental Change. PALAIOS (17), pp. 449-471

Duval-Arnould, A. (2019) Controls on stratigraphic development of shelf margin carbonates: Jurassic Atlantic margin – Essaouira-Agadir Basin, Western Morocco: PhD Thesis, University of Manchester, 287p.

Embry, AF., Klovan, J. E. (1971) A late Devonian reef tract on northeastern Banks Island, N.W.T. Bulletin of Canadian Petroleum Geology 19 (4), 730–781.

Erba, E., Bartolini, A and Larson, R.L. (2004) Valanginian Weissert oceanic anoxic event. Geology (32), 149–152.

Ettachfini, M. (2004) Les ammonites néocomiennes dans l'Atlas atlantique (Maroc): biostratigraphie, paléontologie, paléobiogeographie et paléoécologie. Strata, Mémoire (43), 1–223.

Fernández-Blanco, D., Gouiza, M., Charton, R., Kluge, C., Klaver, J., Brautigam, K and Bertotti, G. (2020) Anticline growth by shortening during crustal exhumation of the Moroccan Atlantic Margin. Eartharxiv (PREPRINT).

Ferry, S., Masrour, M and Grosheny, D. (2007) Le Crétacé de la marge atlantique marocaine (région d'Agadir). Manuscrit auteur publié dans Excursion du Groupe Français du Crétacé Série "Excursion" 75 p.

Flügel, E. (2004) Microfacies of Carbonate Rocks: Analysis, Interpretation and Application. 2nd edition. Springer, 976.

Föllmi, K.B., Bodin, S., Godet, A., B. van de Schootbrugge and Linder, P. (2007) Unlocking paleo-environmental information from Early Cretaceous shelf sediments in the Helvetic Alps: stratigraphy is the key! Swiss Journal of Geosciences (100), 349-369.

Föllmi, K.B. (2012) Early Cretaceous life, climate and anoxia. Cretaceous Research (35), 230-257.

Garberoglio, R.M and Lazo, D.G. (2014). Coral biostromes from the Hauterivian of the southeastern Pacific, Neuquén Basin, West-Central Argentina. Conference Paper: 4th International Palaeontological Congress, Mendoza, Argentina.

Gale, A.S., Mutterlose, J and Batenburg, S., Gradstein, F.M., Agterberg, F.P., Ogg, J.G and Petrizzo, M.R. (2020) The Cretaceous Period. In: (2020) Gradstein, F.M., Ogg, J.G., Schmitz, M and Ogg, G.M. Geologic Time Scale 2020. Chapter 27.

Godet, A. (2013) Drowning unconformities: Palaeoenvironmental significance and involvement of global processes. Sedimentary Geology (293), 45–66.

Götz, S., Löser, H., Schmid, D.U. (2005) Reef development on a deepening platform: two Early Cretaceous coralgal patch reefs (Catí, Llàcova Formation, eastern Spain) compared. Cretaceous Research (26), 864-881.

Hafid, M., Zizi, M., Bally, A.W., Aït Salem, A. (2006) Structural styles of the western onshore and offshore termination of the High Atlas, Morocco. Comptes Rendus Geoscience (338), 50–64.

Hallock, P and Schlager, W. (1986) Nutrient Excess and the Demise of Coral Reefs and Carbonate Platforms. PALAIOS (1), 389-398.

Insalaco, E. (1996) A Sedimentological and Palaeoecological study of Oxfordian (Upper Jurassic) coral-dominated reefal carbonates in Western Europe. PhD Thesis, University of Birmingham.

Insalaco, E. (1998) The descriptive nomenclature and classification of growth fabrics in fossil scleractinian reefs. Sedimentary Geology (118), 159–186.

Kendall, C.G.S.C., Schlager, W. (1981) Carbonates and relative changes in sea-level. Mar.Geol. (44), 181–212.

Kessels, K., Mutterlose, J and Michalzik, D. (2006) Early Cretaceous (Valanginian - Hauterivian) calcareous nannofossils and isotopes of the northern hemisphere: proxies for the understanding of Cretaceous climate. Lethaia (39).

Kolodziej, B and Bucur, I.I. (2020) An Early Cretaceous mesophotic coral ecosystem built by platy corals (middle Aptian, Southern Carpathians, Romania). Cretaceous Research (109).

Koutsoukos, E and Hart, M.B. (1990) Cretaceous foraminiferal morphogroup distribution patterns, palaeocommunities and trophic structures: a case study from the Sergipe Basin, Brazil. Earth and Envrionmental Science Transactions of the Royal Society of Edinburgh (81), 221-246.

Lathuilière, B., Gaillard, C., Habrant, N and Werner, W. (2005) Coral zonation of an Oxfordian reef tract in the northern French Jura. Facies (50), 545-559.

Le Roy, P., Piqué, A. (2001) Triassic–Liassic Western Moroccan synrift basins in relation to the Central Atlantic opening. Marine Geology (172), 359–382.

Lini, A., Weissert, H and E. Erba, E. (1992) The Valanginian carbon isotope event: A first episode of greenhouse climate conditions during the Cretaceous, Terra Nova (4), 374– 384.

Lokier, S.W., Wilson, M.E.J and Burton, L.M. (2009) Marine biota response to clastic sediment influx: A quantitative approach. Palaeogeography, Palaeoclimatology, Palaeoecology (281), 25-42.

Löser, H. (2009) Morphology, taxonomy and distribution of the Early Cretaceous coral genus Holocoenia (Scleractinia) and its first record in the Caribbean. Revista Mexicana de Ciencias Geológicas (26), 93-103.

Luber, T.L., Bulot, L.G., Redfern, J., Frau, C., Arantegui, A., Masrour, M. (2017) A revised ammonoid biostratigraphy for the Aptian of NW Africa: Essaouira-Agadir Basin, Morocco. Cretaceous Research (79), 12–34.

Luber, T.L., Redfern, J., Nahim, M., Jeremiah, J., Simmons, M., Bodin, S., Frau, C., Bidgood, M and Masrour, M. (2018) A revised chronostratigraphic framework for the Aptian of the Essaouira-Agadir Basin, a candidate type section for the NW African Atlantic Margin. Cretaceous Research (9).

Masse, J.P., Morycowa, E and Masse, M.F. (2009) Valanginian-Hauterivian scleractinian coral communities from the Marseille region (SE France). Cretaceous Research (30), 178-192.

McArthur, J.M., Janssen, N.M.M., Reboulet, S., Leng, M.J., Thirlwall, M.F., B. van de Schootbrugge. (2007) Palaeotemperatures, polar ice-volume, and isotope stratigraphy (Mg/Ca, δ18O, δ13C, 87Sr/86Sr): The Early Cretaceous (Berriasian, Valanginian, Hauterivian). Palaeogeography, Palaeoclimatology, Palaeoecology (248), 391-430.

Mcneil, M., Nothdurft, L., Dyriv, N.J., Webster, J.M and Beaman, R.J. (2020) Morphotype differentiation in the Great Barrier Reef Halimeda bioherm carbonate factory: Internal architecture and surface geomorphometrics. Depositional Rec. Accepted Author Manuscript. doi:10.1002/dep2.122.

Minter, N.J., Buatois, L.A and Mángano, M.G. (2016) The Conceptual and Methodological Tools of Ichnology. In: Mángano M., Buatois L. (eds) The Trace-Fossil Record of Major Evolutionary Events. Topics in Geobiology (39), 1-26.

Mokady, O., Lazar, B and Steinitz, H. (1996) Echinoid Bioerosion as a Major Structuring Force of Red Sea Coral Reefs. Biological Bulletin 190 (3).

Moscardelli, L., Ochoa, J., Lunt, I and Zahm, L. (2019) Mixed siliciclastic–carbonate systems and their impact for the development of deep-water turbidites in continental margins: A case study from the Late Jurassic to Early Cretaceous Shelburne subbasin in offshore Nova Scotia. AAPG Bulletin (103), 2487–2520.

Mutterlose, J., Rawson, P., Reboulet, S., Baudin, F., Bulot, L., Emmanuel, L., Gardin, S., Martinez, M and Renard, M. (2020) The Global Boundary Stratotype Section and Point (GSSP) for the base of the Hauterivian Stage (Lower Cretaceous), La Charce, southeast France. Episodes (44), 129-150.

Olivier, N., Martin-Garin, B., Colombie, C., Cornee, J. J., Giraud, F., Schnyder, J., Kabbachi, B., and Ezaidi, K. (2012) Ecological succession evidence in an Upper Jurassic coral reef system (Izwarn section, High Atlas, Morocco). Geobios (45), 555-572.

Pandey, D.K., Fürsich, F.T., Alberti, M., Sharma, J.K and Swami, N. (2018) Recurrent hardgrounds and their significance for intra-basinal correlations: a case study of upper Bathonian rocks from the western margin of the Indian craton. Journal of Palaeogeography, 7-14.

Pichel, L.M., Huuse, M., Redfern, J and Finch, E. (2019) The influence of base-salt relief, rift topography and regional events on salt tectonics offshore Morocco. Marine and Petroleum Geology (103), 87-113.

Price, G.D. and Mutterlose, J. (2004) Isotopic signals from late Jurassic–early Cretaceous (Volgian-Valanginian) sub-Arctic belemnites, Yatria River, Western Siberia. J. Geol. Soc. London (161) 959-968.

Purkis, S. J. and Harris, P. M. (2016) The Extent and Patterns of Sediment Filling of Accommodation Space on Great Bahama Bank. Journal of Sedimentary Research (86), 294-310.

Rameil, N., Immenhauser, A., Warrlich, G., Hillgärtner, H and Droste, H.J. (2010) Morphological patterns of Aptian Lithocodium–Bacinella geobodies: relation to environment and scale. Sedimentology (57), 883–911.

Reiss, Z and Hottinger, L. (1984) The Gulf of Aqaba: Ecological Micropaleontology. Springer, Berlin, 354p.

Reolid, M., Molina, J.M., Löser, H., Navarro, V and Ruiz-Ortiz, P.A. (2009) Coral biostromes of the Middle Jurassic from the Subbetic (Betic Cordillera, southern Spain): facies, coral taxonomy, taphonomy, and palaeoecology. Facies (55), 575-593.

Rey, J., Canérot, B., Peybernès, B., Taj-Eddine, K., Rahhali, I., Thieuloy, J.-P. (1986a) Le Crétacé inférieur de la région d'Essaouira: données biostratigraphiques et évolutions sédimentaires. Revue de la Faculté des Sciences de Marrakech, Numéro spécial (2), 413-411.

Rey, J., Canérot, B., Rocher., A., Taj-Eddine, K., Thieuloy, J.-P. (1986b) Le Crétacé inférieur sur le versant nord du Haut-Atlas (région d'Imi n'Tanout et Amizmiz) données biostratigraphiques et évolutions sédimentaires. Revue de la Faculté des Sciences de Marrakech, Numéro spécial (2), 393-441.

Rey, J., Canérot, J., Peybernès, B., Taj-Eddine, K., Thieuloy, J-P. (1988) Lithostratigraphy, biostratigraphy and sedimentary dynamics of the Lower Cretaceous deposits on the northern side of the western High Atlas (Morocco). Cretaceous Research (9) 141–158.

Rey, J and Dinis, J. (2004) Shallow marine to fluvial Lower Cretaceous of central Portugal: sedimentology, cycles and controls Pre-Meeting Field Trip A5. Cretaceous and Cenozoic events in West Iberia margins. 23rd IAS Meeting of Sedimentology Field Trip Guidebook (2).

Reymond, C.E., Zihrul, K-S., Halfar, J., Riegl, B., Humphreys, A and Westphal, H. (2016) Heterozoan carbonates from the equatorial rocky reefs of the Galápagos Archipelago. Sedimentology (63), 940–958.

Ricci, C., Lathuilière, B and Rusciadelli, G. (2018) Coral communities, zonation and paleoecology of an Upper Jurassic reef complex (Ellipsactinia Limestones, Central Apennines, Italy). Research in Paleontology and Stratigraphy (124), 433-508.

Riegl, B and Piller, E.W. (1997) Distribution and environmental control of coral assemblages in northern Safaga Bay (Red Sea, Egypt). Facies (36), 141-162.

Riegl, B and Piller, E.W. (2000) Reefs and coral carpets in the northern Red Sea as models for organism-environment feedback in coral communities and its reflection in growth fabrics. In:

Insalaco, E., Skelton, P.W and Palmer, T.J. (2000). Carbonate Platform Systems: components and interactions. Geological Society, London, Special Publications (178), 71-88.

Rogov, A.M., Ershova, V.B., Shchepetova, E.V., Victor, A., Zakharov, A., Pokrovsky, B.G and Khudoley, A.K. (2017) Earliest Cretaceous (late Berriasian) glendonites from Northeast Siberia revise the timing of initiation of transient Early Cretaceous cooling in the high latitudes. Cretaceous Research (71), 102-112

Rosen, B.R; Aillud, G.S; Bosellini, F.R; Clack, N.J; Insalaco, E; Valldeperas, F.X. and Wilson, M.E.J. (2000) Platy coral assemblages: 200 million years of functional stability in response to the limiting effects of light and turbidity. Proceedings 9th International Coral Reef Symposium, Bali, Indonesia.

Sandberg, P.A. (1983) An oscillating trend in Phanerozoic non-skeletal carbonate mineralogy. Nature (305), 19–22.

Sanders, C., Baron-Szabo, R.C. (2005) Scleractinian assemblages under sediment input: their characteristics and relation to the nutrient input concept. Palaeogeography, Palaeoclimatology, Palaeoecology (216), 139-181.

Schlager, W. (2003) Benthic carbonate factories of the Phanerozoic. Int J Earth Sci (Geol Rundsch) (92), 445–464.

Schlagintweit, F and Bover-Arnal, T. (2010) New insights into Lithocodium aggregatum Elliott 1956 and Bacinella irregularis Radoičić 1959 (Late Jurassic–Lower Cretaceous): two ulvophycean green algae (?Order Ulotrichales) with a heteromorphic life cycle (epilithic/euendolithic). Facies (56), 509-547.

Schmid, D.U and Leinfelder, R.R. (1996) The Jurassic Lithocodium Aggregatum – Troglotella Incrustans Foraminiferal Consortium. Palaeontology (39), 21-52.van de Schootbrugge, B., Föllmi, K.B., Bulot, L.G., and Burns, S.J. (2000) Paleoceanographic changes during the Early Cretaceous

(Valanginian- Hauterivian): Evidence from oxygen and carbon stable isotope: Earth and Planetary Science Letters (181), 15–31.

Scotese, C.R. (2014) Atlas of Early Cretaceous Paleogeographic Maps, PALEOMAP Atlas for ArcGIS, volume 2, The Cretaceous, Maps 23 - 31, Mollweide Projection, PALEOMAP Project, Evanston, IL.

Scotese, C.R., Song, H., Mills, B.J.W and van der Meer, D.G. (2021) Phanerozoic paleotemperatures: The earth's changing climate during the last 540 million years. Earth-Science Reviews (215).

Scott, R.W and Aleman, A. (1984) Stylina columbaris n. sp. in a Lower Cretaceous Coral Biostrome, Peru. Journal of Paleontology (58), 1136-1142.

Sikharulidze, G. (1979) The corals of the Urgonian facies of Georgia. Geobios (12) Supplement 1, 301 30.

Simmons, M., Miller K.G., Ray, D.C., van Buchem, F.S.P and Gréselle, B. (2020) Phanerozoic Eustasy. In: (2020) Gradstein, F.M., Ogg, J.G., Schmitz, M and Ogg, G.M. Geologic Time Scale 2020. Chapter 13.

Tari, G and Jabour, H. (2013) Salt tectonics along the Atlantic margin of Morocco. Geological Society, London, Special Publications (369). 337–353.

Taylor, K.G and Macquaker, J.H.S. (2000) Early diagenetic pyrite morphology in a mudstone-dominated succession: the Lower Jurassic Cleveland Ironstone Formation, eastern England. Sedimentary Geology (121), 77-86.

Tomas, S., Löser, H and Salas, R. (2008) Low-light and nutrient-rich coral assemblages in an Upper Aptian carbonate platform of the southern Maestrat Basin (Iberian Chain, eastern Spain). Cretaceous Research (29), 509–534.

Tucker, M.E and Wright, P. (1980) Carbonate Sedimentology. Wiley-Blackwell 498p.

Tucker, M.E. (2003) Mixed Clastic–Carbonate Cycles and Sequences: Quaternary of Egypt and Carboniferous of England. Geologia Croatica (56), 19-37.

Vescogni, A., Bosellini, F.R., Cipriani, A., Gürler, G., Ilgar, A and Paganelli, E. (2014) The Dağpazarı carbonate platform (Mut Basin, Southern Turkey): Facies and environmental reconstruction of a coral reef system during the Middle Miocene Climatic Optimum. Palaeogeography, Palaeoclimatology, Palaeoecology (410), 213-232.

Wells, J.W. (1946) Some Jurassic and Cretaceous corals from Northern Mexico. Paleontology (20), 1-7.

Westphal, H., Halfar, J. and Freiwald, A. (2010) Heterozoan carbonates in subtropical to tropical settings in the present and past. Earth Science (99), 153–169.Wippich, M. (2001) Valanginian (Early Cretaceous) ammonite faunas from the western High Atlas, Morocco, and the recognition of western Mediterranean 'standard' zones. Cretaceous Research 24 (4), 357-374.

Witam, O. (1998) Le Barrémien-Aptien de l'Atlas Occidental (Maroc): lithostratigraphie, biostratigraphie, sédimentologie, stratigraphie séquentielle, géodynamique et paléontologie. Strata (30), 1–421.

Wright, P and Burgess, P.M. (2005) The carbonate factory continuum, facies mosaics and microfacies: an appraisal of some of the key concepts underpinning carbonate sedimentology. Facies (51), 17–23.

Zawada, K.J.A., Dornelas, M and Madin, J.S. (2019) Quantifying coral morphology. Coral Reefs (38), 281-1292.

Zeller, M., Verwer, K., Eberli, G., Massaferro, J.L., Schwarz and Spalletti, L. (2016) Depositional controls on mixed carbonate-siliciclastic cycles and sequences on gently inclined shelf profiles. Sedimentology (62), 2009-2037.

Section ID	Latitude (°)	Longitude (°)	Elevation (m)
TAM1	30.742878	-9.713569	143
TAM2	30.740083	-9.718569	150
TAM3	30.735633	-9.726003	190
TAM4	30.72505	-9.723519	193
TAM5	30.741653	-9.738289	201
TAM6	30.743508	-9.736031	180
TAM7	30.744631	-9.7331	176
TAM8	30.742078	-9.72705	175
TAM9	30.714539	-9.684558	220
TAM10	30.744806	-9.701525	138
AMS-1	31.0977	-9.816494	95

TABLE 1

Lithofacies	Textures	Skeletal Abundance	Sedimentary Structures	Bed Thickness (cm)	Cementation/Mineralisation	Non-skeletal component	Facies Association	Process Interpretation	Facies Code
Bioclastic siltstone to sandstone	Grain-supported	Oysters (usually at base), serpulids, bivalves, brachiopods, bryozoans, echinoids and small elongated shell fragments	Planar to wavy laminations, moderately to intensely bioturbated top surface (and up to 20 cm below (Thalassinoides, Trypanites, Skolithos). Thin fragments orientated NNW-SSE. Sharp and irregular basal surfaces	10 to 120	Blocky calcite cement, small patches of micrite common, framboidal pyrite rare	Abundant poorly-moderately sorted sub-angular silt to fine sand-sized quartz	Shoreface	Fairly rapid deposition, unidirectional flow, mixing of siliciclastics with wave-reworked bioclasts	A.1
Laminated siltstone to sandstone	Grain-supported	Occasional small shell fragments	Horizontal, wavy and cross-laminations common with moderately bioturbated (thalass', trypanites) top surfaces. Usually sharp based	2 to 40	Fibrous cement in shell remains, iron oxide crusts on bed tops	Abundant well sorted silt to fine well-sorted sand-sized quartz	Shoreface	Fairly rapid deposition, bi-directional flow with periodic changes in energy leading to ripple migration	A.2
Sandy packstone to grainstone	PST-RST	Oysters, echinoids, gastropods, serpulids, bivalves, brachiopods, bryozoans, coral frags, rare ammonoids	Moderate bioturbation (thalass', trypanites, skolithos) undulating to sharp bases which may have shell lag (usually oysters)	20 to 100	Fibrous to blocky calcite cement and micrite in matrix common, iron oxide minerals in skeletal fragments and crusts	Common sub-angular, poorly sorted silt to very fine sand-sized quartz	Inner platform	Relatively high energy, bioclast reworking and mixing with quartz, intervals of low energy allowing moderate bioturbation	B.1
Silty wackestone to grainstone	WST-GST	Oysters, echinoids, gastropods, serpulids, bivalves, brachiopods, bryozoans, coral frags and rare ammonoids and rare stromatoporoids	Uncommon horizontal lamination in silt-rich intervals, undulating to sharp bases and occassional shell fragment clusters orientated NNW-SSE. Moderate to intense bioturbation (thalass', trypanites, skolithos)	10 to 120	Fibrous (can be syntaxial), blocky calcite and microspar cement common, iron oxide mineralisations and surface crusts abundant	Common sub-angular and poorly sorted silt-sized quartz	Inner platform	Moderate energy, bioclast reworking and mixing with silt-sized quartz, intervals of low energy allowing moderate bioturbation	B.2
Oyster floatstone	MST-WST	Oysters (up to 10cm diameter and thick-shelled) usually fragmentary, serpulids, brachiopods and bivalves	Poorly consolidated and nodular beds common. Moderately to intensely bioturbated (thalassinoides common)	10 to 100	Common microspar cement, iron oxide enriched skeletal fragments and crusts abundant	Common sub-angular and poorly sorted silt-very fine sized sand	Inner platform	Reworked from nearby oyster-banks and deposited in muddy environments during episodic storm events	C

Coral domestone	WST-RST	Densely-packed-branching corals up to 100cm in diameter, dome-lenticular shape). Subordinate undiff' massive shaped corals. Oysters, red algae, bryozoans, echinoids, brachiopods, bivalves, serpulids and *Lithocodium aggregatum*, benthic foraminifera	Beds can be continuous or nodular with bases commonly undulating. Can be moderately to intensely bioturbated (thalass, trypanites, skolithos) and encrusting organisms common. Non-planar base to individual corals	10 to 500	Blocky (can be twinned), fibrous calcite and microspar cements as patches in matrix or in remains, calcite vuggy, iron oxide minerals common	Uncommon to common sub-angular, poorly sorted silt to very fine sand-sized quartz	Inner platform (well-lit, high energy)	Shallow (5-10m WD), moderate-high energy. Corals forming on hard substrates. Changing energy and sedimentation rate allowing varied morphology and varying bioturbation, mixed inter-coral sediment of mud, quartz and reworked bioclasts	D.1
Coral plateston e	WST-RST	Similar assemblage to D.1 with platy/flat corals being the dominant coral and subordinate thin and small ramose branching corals	Beds can be semi-continous and lenticular with moderate to intense bioturbation and bio-encrustations are common. Non-planar base to individual corals	1 to 50	Blocky (can be twinned), fibrous calcite and microspar cements as patches in matrix or in remains, calcite vuggy, iron oxide minerals common,	Uncommon sub-angular, poorly sorted silt to very fine sand-sized quartz	Middle platform (poorly-lit, turbid)	Relatively shallow (10-30m WD) and low to moderate energy, corals forming on hard substrates between muddy sediment. Changing energy allowing varying bioturbation rates	D.2
Bioclastic wackestone to packestone	MST-WST	Oysters, brachiopods, bivalves, serpulids, echinoids, bryozoans, gastropods, rare belemnites, rare small tabular corals and coral fragments	Beds can be nodular and have undulating to relatively sharp bases, slight to intense bioturbation (thalassi, skolithos) especially on bed tops	5 to 120	Blocky-fibrous calcite (can be twinned), microspar cement (both in remains and in matrix), vuggy calcite, iron oxide enriched skeletal remains abundant, framboidal pyrite	Uncommon to rare sub-angular poorly sorted silt to very fine sand-sized quartz	Inner to middle platform	Low to moderate energy, bioclast reworking, intervals of low energy allowing bioturbation and larger reworked bioclasts deposited during increased energy (e.g. storm events)	E
Calcareous mudstone	MST	Small oysters, other bivalves, brachiopods, rare ammonoids and undiff' shell fragments and rare nannfossils and forams	No bedding structures and abrupt changes in lateral continuity. Can be nodular in appearance	5 to over 500	Microsparite cement, iron enriched skeletal fragments and nodules common (typically pyrite)	Uncommon to rare silt-sized quartz	Outer platform	Suspension fall-out, pelagic sedimentation and minor disturbances with reworked bioclasts	F

TABLE 2

Kilometre-scale coral carpets on mixed carbonate-siliciclastic platforms; a sedimentological study from the Lower Cretaceous of northwest Africa

Orrin Bryers[1], Luc Bulot[2, 1], Aude Duval-Arnould[1], Cathy Hollis[1] & Jonathan Redfern[1]

1 – Department of Earth and Environmental Sciences, University of Manchester

2 – Laboratoire Géosciences Océan – LGO, UMR6538 CNRS-UBO-UBS

Highlights

- Kilometre-scale coral-rich outcrops onshore the Moroccan Atlantic Margin
- Non-framework coral carpets show no internal zonation
- Coral morphology and abundance controlled chiefly by water energy and turbidity
- Establishment and demise of corals linked to sea level and climatic change
- Low diversity corals possible proxy for recovery/loss in response to environmental stress

Declaration of interests

☒ The authors declare that they have no known competing financial interests or personal relationships that could have appeared to influence the work reported in this paper.

☒The authors declare the following financial interests/personal relationships which may be considered as potential competing interests: